Synthesis and evaluation of a charge sensitive amplifier for neutron counters

S Strachan
23352108

Dissertation submitted in partial fulfillment of the requirements for the degree *Magister Engineering* in Electric-, Electronic & Computer Engineering at the Potchefstroom Campus of the North-West University

Supervisor: Prof J.E.W. Holm
Co-supervisor: Prof H. Moraal

November 2013

The financial assistance of the National Research Foundation (NRF) towards this research is hereby acknowledged. Opinions expressed and conclusions arrived at, are those of the author and are not necessarily to be attributed to the NRF.

Acknowledgements

I would like to thank the following people for making this project possible:

Prof JEW Holm

Prof H Moraal

Prof PH Stoker

Prof E Nordlander

Mr B Visser

All glory to God

Abstract

Cosmic-ray fluctuations are monitored by neutron monitors using several different kinds of proportional counter tubes. An important component of these monitors is the electronic subsystem that registers and counts output pulses from these counter tubes. Part of the electronic subsystem is a specific preamplifier. The pulse-height distribution curve of the existing preamplifier used in the neutron monitor system at the Centre for Space Research at the North-West University was found to be incorrect, and therefore the pulse-height information cannot be used for further research on the counter tube characteristics. A correct pulse-height distribution implies that the envelope of the pulse, as generated by an amplifier, has a very specific shape as a result of the physics that governs the generation of pulses in the neutron counter tube. It was therefore proposed that a new charge-sensitive preamplifier be synthesized to provide an output that provides the correct pulse-height distribution graph for a neutron monitor system.

The Centre for Space Research at the North-West University is in the process of designing and building a new mini neutron monitor system. The new charge-sensitive preamplifier will be implemented into this updated system. Ultimately, the electronic subsystem must be able to provide a pulse-height distribution graph at the push of a button, thus making the preamplifier a key component in the new design.

In this dissertation the theory of charge-sensitive amplifiers is researched following a design science research methodology. The results showed that a charge-sensitive amplifier can be synthesized to address both the real-world requirements and the theoretical requirements of this research.

Keywords: neutron monitor, charge-sensitive amplifier, preamplifier, design science research, research, design

Uittreksel

Fluktuasies van kosmiese strale word gemoniteer deur neutronmonitors met behulp van verskillende soorte proporsionele telbuise. 'n Belangrike komponent van hierdie monitors is die elektroniese substelsel wat die telbuise se uitsetpulse registreer en tel. Deel van die elektroniese substelsel is 'n spesifieke voorversterker. Die pulshoogte-verdelingskromme van die bestaande voorversterker wat deur die Sentrum vir Ruimtenavorsing by die Noordwes-Universiteit gebruik word, is nie korrek nie en daarom kan die pulshoogte-inligting nie gebruik word vir verdere navorsing op die telbuiseienskappe nie. 'n Korrekte pulshoogteverdeling impliseer dat die omhulsel van die puls, soos gegenereer deur 'n versterker, 'n baie spesifieke vorm het, gebaseer op die fisika wat die opwekking van pulse in die neutrontelbuis reguleer. Die navorsingsvoorstel was dat 'n nuwe ladingsensitiewe voorversterker gesintetiseer moes word om 'n uitset te voorsien wat die korrekte pulshoogteverdelingsgrafiek vir 'n neutronmonitor stelsel sal lewer.

Die Sentrum vir Ruimtenavorsing by die Noordwes-Universiteit is in die proses om 'n nuwe mini neutronmonitor stelsel te ontwerp en bou. Die nuwe ladingsensitiewe voorversterker sal in die opgedateerde sisteem geïmplementeer word. Uiteindelik moet die elektroniese substelsel in staat wees om 'n pulshoogteverdelingsgrafiek met die druk van 'n knoppie te lewer. Daarom is die voorversterker baie 'n belangrike komponent in die nuwe ontwerp.

Die teorie van ladingsensitiewe versterkers is nagevors deur gebruik te maak van ontwerpsnavorsingswetenskap (“design science research”). Die resultate toon aan dat ‘n ladingsensitiewe versterker ontwerp kan word om beide die werklike vereistes sowel as die teoretiese vereistes van die navorsing aan te spreek.

Sleutelwoorde: neutron monitor, ladingsensitiewe versterker, voorversterker, ontwerpwetenskap, navorsing, ontwerp

List of abbreviations and acronyms

$^{10}BF_3$ - Boron trifluoride

BJT - bipolar junction transistor

CMR - common-mode rejection

DSR - design science research

ENC - equivalent noise charge

eV - electron volt

FET - field-effect transistor

FWHM - full width half max

^{3}He - Helium-3

HV - high voltage

IC - integrated circuit

PC - personal computer

PCB - printed circuit board

PSU - power supply unit

SMD - surface mount device

Table of Contents

List of Figures

1. Introduction

In this chapter the problem statement and context of the project are discussed. The objectives and scope of the project are defined. To conclude this chapter, an overview of the thesis is given.

1.1 Overview

Cosmic-ray fluctuations are monitored by neutron monitors using several different kinds of proportional counter tubes. An important component of these monitors is the electronic sub-system that registers and counts output pulses from these counter tubes. In the current neutron monitoring system used by the Centre for Space Research at the North-West University, many of the electronic sub-systems and modules date back to more than a decade ago and have become outdated. The Centre for Space Research at the North-West University is currently in the process of designing and building a new mini neutron monitor system. The new system will use upgraded electronics and makes use of a microprocessor for registering and counting pulses.

Part of the electronic subsystem is a charge-sensitive preamplifier – this amplifier is at the core of this research. Output pulses from the counter tubes need to be conditioned and amplified sufficiently such that they can be recorded and counted. This makes the preamplifier system a key component of the neutron monitor.

The preamplifier that is currently used in the neutron monitor system amplifies the pulses sufficiently to be counted, but it does not provide a correct pulse-height distribution. A correct pulse-height distribution implies that the envelope of the pulse, as generated by a charge-sensitive amplifier, has a very specific shape as a

result of the physics that govern the generation of pulses in the neutron counter tube. The current pulse-height distribution graph (blue) superimposed on the expected/correct pulse-height distribution (black) is shown in Figure 1. The correct pulse-height distribution of a neutron counter tube is discussed in Chapter 3.

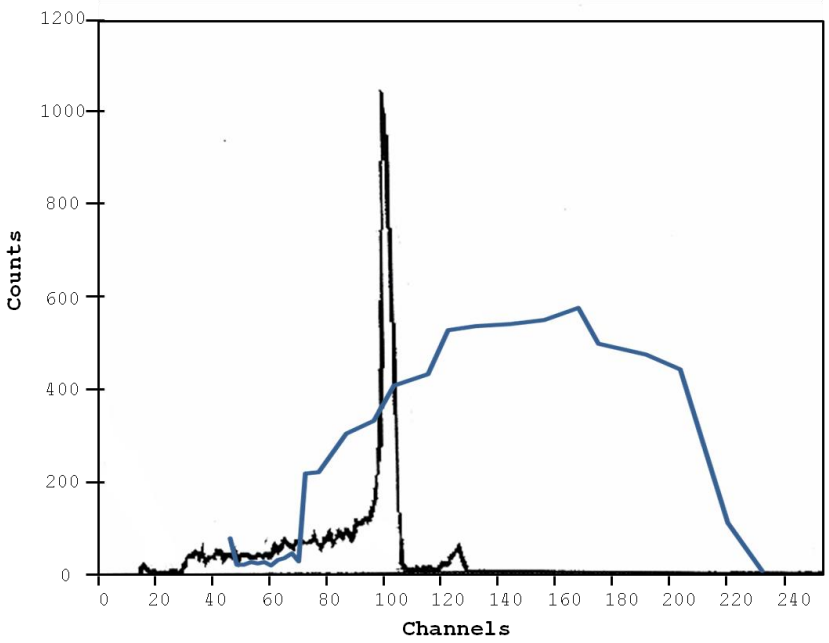

Figure 1: Current results superimposed on datasheet pulse-height distribution graph

A new preamplifier will, therefore, be implemented into this updated neutron monitor system. Ultimately, the system must be able to provide a pulse-height distribution graph at the push of a button, thus making the preamplifier a key component in the new design. This pulse-height distribution will be used to monitor counting rates and sensitivity of the proportional counter tubes used by the Centre for Space Research.

We formally state the research problem as follows:

Is it possible to synthesize an effective charge-sensitive amplifier, from first principles, that addresses the real-world requirements of a neutron monitor system used at the Centre for Space Research of the North-West University?

The solution to the above research problem is thus to (i) research, (ii) synthesize and (iii) evaluate a charge-sensitive preamplifier, also known as an integrating amplifier, for a neutron monitor system.

1.2 Scope of study

Research, synthesis, and evaluation form part of this study. As there are many possible approaches to solving the research problem, a thorough literature study was done to define the characteristics of the new charge-sensitive preamplifier.

The real-world artefact of this research is a functionally capable charge-sensitive preamplifier that can be integrated into a neutron monitor system to provide a correct pulse-height distribution graph for a neutron counter.

In order for the above outcome to be reached, the following *methodology* must be followed:

- Define the real-world problem: Derive real-world requirements so that the artefact can be integrated into a larger neutron monitor system;
- Identify an appropriate research methodology to find a suitable solution: Both theory and practice must be considered when performing this research;
- Study literature related to charge-sensitive amplifiers: A new amplifier must be synthesized from first principles and proper research must be done to understand the underlying theoretical principles and technology;
- Synthesize and construct the real-world artefact: The result of this research must be a functionally capable artefact;
- Evaluate the synthesized artefact: Through simulation and testing, ensure that the correct design decisions were made and that the artefact is functional.

1.3 Overview of thesis

A design science research (DSR) methodology was selected as it provided the most appropriate research framework, as DSR provides a framework for both theoretical and practical research and outputs. When following a DSR methodology, a theoretical problem is identified (in a sense, translated) from the real-world problem and used to formulate a theoretical research question. More details on DSR are provided in Chapter 2.

The theoretical problem is investigated through an extensive literature research, in this case a study on neutron monitors, pulse-height distribution of proportional counter tubes, amplifiers in general, and charge-sensitive amplifiers. Using the knowledge obtained from the literature study, as well as the inputs of an expert in amplifier design for neutron monitors, a real-world artefact is synthesized through simulations – this artefact is the charge-sensitive amplifier.

Simulations are used extensively in the design and characterisation of the amplifier. After satisfactory results have been obtained from simulations, the amplifier is constructed and evaluated in a neutron monitor test setup.

Experiments are conducted to answer the ***research question***, namely to answer the question:

Is it possible to synthesize an effective charge-sensitive amplifier, from first principles, that addresses the real-world requirements of a neutron monitor system used at the Centre for Space Research of the North-West University?

Empirical results from simulations and measurements are evaluated to ascertain whether a pulse-height distribution graph with shape similar to specifications as provided by neutron tube manufacturers can be obtained. ***Validation*** is achieved when all real-world requirements as specified by the neutron monitor system have been addressed. ***Verification*** is achieved when selected empirical measurements match simulation results as well as the theoretical results found in the datasheet of the counter tube.

2. Research methodology

This chapter illustrates the use of design science research as a method for synthesis and evaluation of a charge-sensitive amplifier for a neutron monitor system.

2.1 Introduction

A design science research method was followed in this research. The following two sections provide a description of the DSR process and how it was used in this research.

2.2 Overview of design science research

Design is fundamental to the information systems discipline, the contributions of new performance in the development and use of information systems [1]. Instantiations or implementations demonstrate the feasibility of utilizing artefacts for a given task. They are evaluated with respect to their effectiveness and efficiency in the performance of the given task. Although DSR has been applied mostly to information technology, DSR principles were also found to be very effective in engineering research that also produced an artefact as part of research [2].

A design science research contribution requires the following [3]:

1. Identification and clear description of a relevant organizational problem;
2. Demonstration that no (obviously) adequate solutions exist in the extant knowledge-base;
3. Development and presentation of a novel artefact (constructs, models, methods or instantiations) that addresses the problem;
4. Rigorous evaluation of the artefact enabling the assessment of its utility;
5. Articulation of the value added to the knowledge-base and to practice;
6. Explanation of the implications for management and practice.

The design science research process can also be described as in Figure 2.

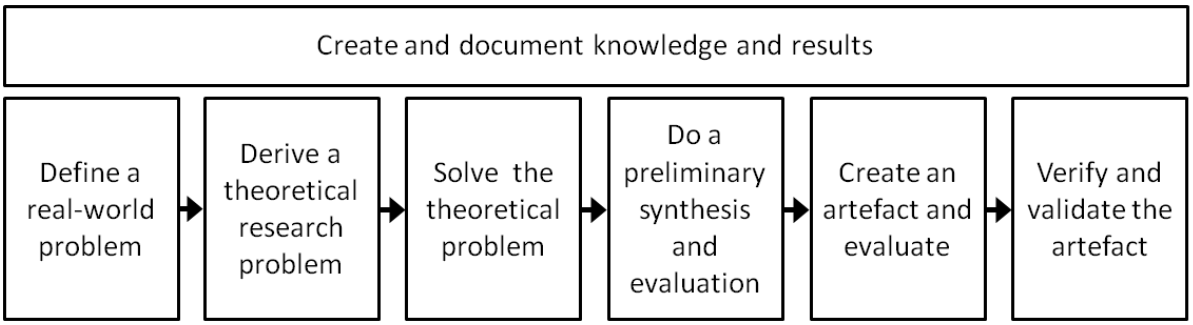

Figure 2: Block diagram of design science research procedure [4]

2.3 DSR methodology applied to this research

Figure 3 shows how the design science research procedure was used in this project.

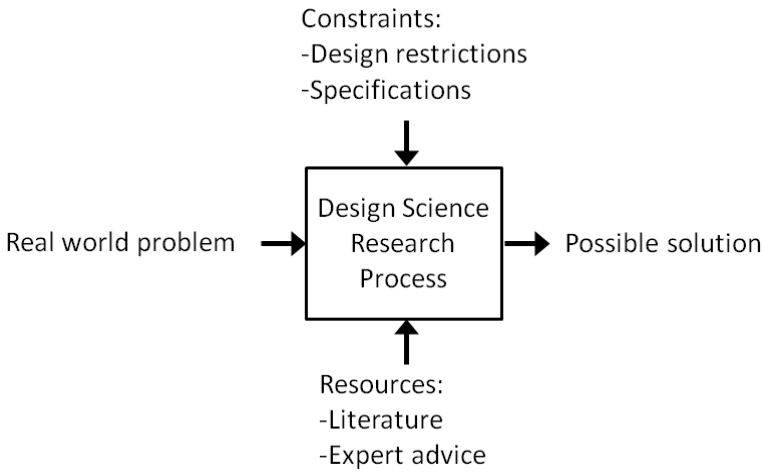

Figure 3: DSR implemented in this project [4]

The literature study and constraints of the design will be discussed in detail in Chapter 3 and Chapter 4 respectively.

2.3.1 Design Science Research process for this project

Real-world problem:

The neutron monitor preamplifiers, currently being used by the Centre for Space Research at the North-West University, produce an incorrect pulse-height distribution. The result is that this pulse-height distribution data cannot be used to investigate the possibility of drift on the counter tubes.

After the evaluation and testing of the existing neutron monitor system preamplifiers, it was noticed that, even though these preamplifiers have sufficient amplification of pulses received from the neutron monitor counter tube to register the pulses, they amplify the input voltage of each pulse received instead of amplifying the accumulated charge that each neutron occurrence deposits on the counter tube anode wire. This results in an incorrect pulse-height distribution graph for the counter tube.

Theoretical research problem:

A design model for a charge amplifier, suitable for neutron monitor application, did not exist at the onset of this research. A literature study on neutron monitor systems, pulse-height distributions of neutron monitors, amplifiers, preamplifiers, and charge amplifiers revealed that, although options exist in practice, a model with sufficient design flexibility was not available.

In order to define the theoretical research problem, a research question was formulated, namely to investigate the possibility of synthesizing a charge-sensitive preamplifier that adheres to the requirements of the Centre for Space Research at the North-West University. The solution to the research problem is to (i) research, (ii) synthesize and (iii) evaluate a charge-sensitive preamplifier, also known as an integrating amplifier, for a neutron monitor system.

Solution of theoretical problem:

From the literature study it was found that a charge-sensitive preamplifier would be the best type of preamplifier to use in a neutron monitor system in order to obtain the correct pulse-height distribution.

A list of objectives was created in order to assist in setting the requirements and constraints for the design of the amplifier.

Objectives:

In order to design a charge-sensitive amplifier as defined in the research question, the following secondary objectives must be addressed:

1. Obtain different possible configurations of charge-sensitive preamplifiers;
2. Define and meet a set of requirements that define the amplifier's characteristics:
    a. Pulse amplification requirements – the preamplifier must amplify charge, with the voltage output of the preamplifier proportional to the total charge on the proportional tube's detector wire. The total integrated charge will typically be 3.3 pC as determined from measurements at the Centre for Space Research. The gain of the preamplifier must be constant and the output should be 35 mV ± 2mV. External gain will be added afterwards to provide a voltage that can be accurately digitized by a microcontroller (the external gain element was not part of the scope of this research) ;
    b. Electrical interface requirement – the input impedance of the preamplifier must meet the counter tube interface requirements so as not to load the counter tube. The output pulse must be 35 mV ± 2mV for an input of 3.3 pC as for the existing preamplifier and counter tubes used. The shaping amplifiers that follow the preamplifier are calibrated during manufacturing. Hence, the output voltage of the preamplifier is not critical in terms of its accuracy.
    c. Power supply requirements (voltage) – the preamplifier must operate on the existing power supply for legacy reasons. The current consumption should be less than 10 mA;

d. Noise characteristics – a low-noise design must be done to ensure acceptable noise performance. This is a design requirement, and an appropriate low-noise amplifier configuration must be selected from literature, with sufficient evidence that the selection is acceptable;
e. Linearity – the preamplifier must be linear inside the operating region. This is a design requirement that must be met as non-linearity will result in an incorrect pulse-height distribution. The amplifier must be linear for different pulse durations and a constant input charge of 3.3 pC;
f. Rise time and decay time – realistic rise and fall times must be provided so that the preamplifier operates in realistic conditions. The input pulse will have a rise time of no less than 1 μs and a decay time of no longer than 300 ms, with the total charge as defined in (a);
g. Defined temperature characteristics – the preamplifier must exhibit acceptable temperature characteristics for use in a controlled neutron monitor environment. That is, an operating range of 25 °C ± 10 °C is required. As the neutron counter measures temperature and can provide temperature correction, it is not a requirement to provide constant gain across the temperature range, but rather to provide the characteristics of the preamplifier across the required range;
h. Physical form factor and interface requirements – in order to interface with existing sub-systems such as the counter tube and counting circuitry, the physical form factor must match the existing form factor;
i. Cost and availability – it is imperative that a solution must be provided using components that are available and affordable. No special purpose devices should be used as the preamplifier will be in service globally and long procurement lead times and unavailability constraints are not acceptable.

3. Implement a configuration that can be verified with simulations and tests against the required characteristics;
4. Validate the amplifier by integrating it into a test setup of the existing sub-systems that make up the neutron monitor.

Preliminary synthesis and evaluation:

From the literature, and with design support of an expert in amplifier design for neutron monitors, design and simulate a low-noise charge-sensitive amplifier.

Create an artefact and evaluate:

Build the designed charge amplifier and implement this amplifier in a neutron monitor test setup.

Verify and validate the artefact:

Evaluate experimental results to ensure that the real-world requirements are met and experimental results match simulation results.

2.4 Verification and validation

Since the charge-sensitive amplifier will be used in a real-world application, the design needs to address the requirements as obtained from an analysis of the real-world problem. This means that the amplifier must address the requirements as specified by the neutron monitor system. By addressing the real-world requirements, the charge-sensitive amplifier artefact is validated – that is, the correct preamplifier was synthesized [5].

The characteristics of the physical charge-sensitive amplifier should be determined by conducting experiments. These experiments will also characterise the real-world artefact. Measurements from these experimental setups are used to verify simulation results. Verification will be achieved when physical measurements of the charge-sensitive amplifier's function and performance match simulation and theoretical (datasheet) values [5].

In many instances, one may argue that validation is obtained when physical measurements agree with simulation results from the design. However, in the spirit of design science research, validation is achieved by ensuring a functionally capable artefact results from the research.

2.5 Summary

This chapter illustrated the use of design science research as a method for synthesis and evaluation of a charge-sensitive amplifier for neutron counters.

A theoretical research problem was identified from the defined real-world problem. The solution of the theoretical problem was investigated by using expert advice and existing literature on neutron monitors, amplifiers, and charge-sensitive amplifiers.

A list of objectives was identified in order to assist in setting the specifications and constraints for the design of the amplifier, as outlined in the sections above. A definition of the preliminary synthesis followed with the design and simulation of the charge-sensitive amplifier.

It was stated that the characteristics of the physical charge-sensitive amplifier can be determined by conducting experiments. These experimental results can be used to characterise the real-world artefact. Measurements from the experimental setups can also be used to verify simulation results.

Verification is achieved when the physical measurements of the charge-sensitive amplifier's function and performance match the values found in simulation and theoretical (datasheet) cases, while validation is achieved when the synthesized preamplifier meets the real-world requirements.

3. Literature study

This chapter discusses the topics that were studied to aid in the solution of the theoretical problem, as well as in the synthesis and evaluation process. Technologies that were used in the research project are discussed in this chapter.

3.1 Introduction

In this literature study existing literature applicable to neutron monitors, the new neutron monitor design, neutron monitor pulse-height distributions, amplifiers, and charge-sensitive amplifiers will be studied to aid in the synthesis and design of a preamplifier for a neutron monitor system.

3.2 Neutron monitor principles

During the late 1940s J.A. Simpson discovered that the latitude dependence of nucleonic intensity in the atmosphere is many times that of the ionizing component. The realization of this discovery gave him the inspiration to invent the cosmic-ray neutron monitor that could better exploit the geomagnetic field as a magnetic spectrometer [6].

In the 1950s a standardized cosmic-ray monitor rapidly replaced the ionization chamber as the detector of choice to monitor cosmic radiation variations [7]. By 1951 Simpson had set up five monitoring stations (the first neutron monitor network) from the city of Chicago to the magnetic equator in Peru, allowing him to use the Earth's magnetic field as an analyzer [6].

In 1954 and 1955, a sea-level survey by Rose et al., verified experimentally that the neutron monitor responded better to lower energy primary cosmic rays than a muon monitor [6]. By 1957-1958 (International Geophysical Year) the neutron monitor

network expanded worldwide to 50 stations. In 1964 the IGY network was supplemented with a second generation of neutron monitors which had a much higher count rate, called the NM64, while the original design is called the IGY monitor [6].

Neutron monitors consist of, amongst other components, a special gas-filled proportional counter tube surrounded by a moderator, a lead producer, and a reflector.

The incident nucleon component (protons and neutrons) of the secondary cosmic-ray flux causes nuclear reactions in the lead, and low energy evaporation neutrons are produced. These MeV-neutrons are slowed down to thermal energies by the moderator, and for example in the NM64 about 6% of the MeV-neutrons are finally detected by the proportional counter tubes. The fact that neutrons are detected gives this cosmic-ray detector its name: neutron monitor [8].

The counter tubes in a neutron monitor detect mainly thermal neutrons, i.e. a kinetic energy of about 0.025 eV. The counter gas is usually Boron Trifluoride ($^{10}BF_3$) or Helium-3 (^3He) [8].

A typical $^{10}BF_3$ detector consists of a cylindrical aluminum (brass or copper) tube filled with a $^{10}BF_3$ fill gas at a pressure of 0.2 to 1.0 atmospheres. The boron trifluoride gas accomplishes two things [9]:

- It functions as the proportional fill gas;

- It undergoes a neutron-alpha interaction with thermal neutrons:

$$^{10}B + n \rightarrow Li^7 + \alpha + Q,$$

where Q = 2.31 MeV in 93% of the reactions.

To improve the detection efficiency, the $^{10}BF_3$ is enriched in ^{10}B. Typical enrichments increase the ^{10}B component to 96% (ordinary boron is 20% ^{10}B and 80% ^{11}B) [9].

^3He proportional counters are widely used for the non-destructive assay of nuclear material. In what are known as active counting techniques, the ^3He proportional counters are subjected to partially thermalized neutron fluxes in the order of 10^8 neutrons/cm^{2}s [10].

The relatively high cross section of ^3He for thermal neutrons makes it an attractive material to be used for neutron detection. Helium is an inert gas and is most commonly used in sealed gas proportional counters. The mechanism for the detection of thermal neutrons uses the following $^3He(n,p)H^3$ reaction [10]:

$$He^3 + n\ (Thermal) \rightarrow H^1 + H^3 + Q,$$

where Q = 764 keV.

Aluminium is typically used as the detector (cathode) wall because of its small cross section for neutrons. The anode is almost always a single thin wire running down the axis of the tube [9]. A diagram of a proportional counter tube is shown in Figure 4.

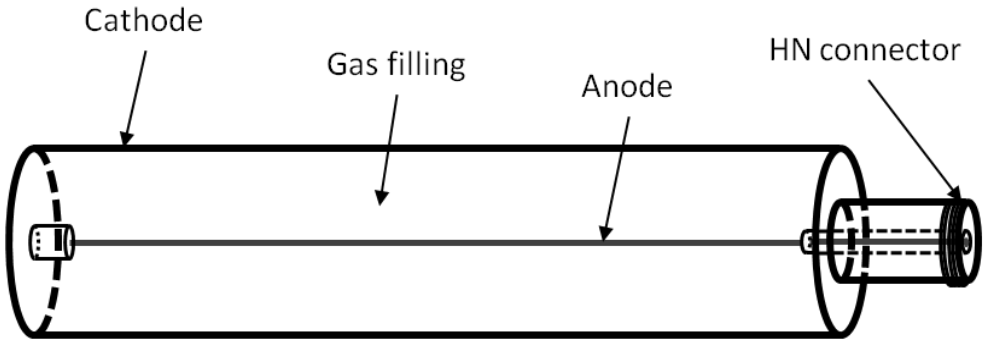

Figure 4: Diagram of a proportional counter tube

Changes in physical dimensions affect the counting rate and sensitivity of the counter tube. Specific datasheets for each tube can be obtained from the designers and

manufacturers, LND Incorporated [11]. The Centre for Space Research at the North-West University uses both $^{10}BF_3$ and ^{3}He counter tubes.

The theory of operation of the counter tube stems from the interaction of the incident radiation with the detector's gas filling, creating ion pairs. Electrons are accelerated toward the anode under the influence of an electric field. As electrons move toward the anode, they collide with neutral gas molecules. Some of these collisions will have sufficient energy to create more ion pairs. The secondary electron generation from collision amplifies the electron signal at the anode, which leads to a larger output pulse. A proportional counter is operated so that the output pulse size is proportional to the initial number of ion pairs. The number of output pulses provides information as to the amount of incident particles, and the size of the pulses provides information as to the energy of these particles [12].

The ratio of the charge collected at the anode compared to the charge from the initial ion pair creation is called gas gain or multiplication. For proportional counters, the operating voltage is adjusted to obtain the desired gas gain. Proportional counters are high-voltage devices, mostly requiring between 1000 and 3000 volts to operate. They require, however, little power, so low current (approximately 1mA) power supplies can be used [12].

An important characteristic of proportional counters is the resolution of the full energy peak, usually measured on a multichannel analyser. In an ideal case, pulses caused by mono-energetic radiation would all be the same height, and the multichannel analyser would display a single line that would represent the radiation energy. In practice, a peak with a measurable width is observed. There are several contributing factors to the width of the energy peak, including statistical variations, detector geometry, gas purity, and electronic noise. The statistical variations set a maximum possible resolution for a given geometry [12].

The electronic noise contribution can be limited by careful selection of electronic components and by limiting stray capacitances. It is desirable to keep the distance between the detector and the preamplifier as short as possible. The detector and electronics should be shielded from electrical interference and well grounded in order to exclude extraneous noise from the counting system. Care should be taken when handling detectors and electronics to avoid noise due to contamination [12].

3.3 New neutron monitor architecture

A new neutron monitor system is currently in the process of being designed and built at the Centre for Space Research at the North-West University. This new neutron monitor system will be much smaller than previous systems. Due to technological advances in electronic components, the entire pulse registration and counting system will be redesigned and will make use of a microprocessor rather than the discrete components previously employed.

The electronic subsystem will consist of a preamplifier, registration and counting system, pressure and temperature sensors, global positioning system (GPS), and a power supply that provides power to both the tube and the electronics. The entire electronic subsystem will be designed to fit in a 200 x 150 x 150 mm box attached to the body of the neutron monitor.

The preamplifiers used in the existing NM64 neutron monitors were factory produced in the 1970s. These were presumed to be functioning optimally. In 2003, new preamplifiers were designed for the mini neutron monitors. These amplifiers were found to be sensitive enough, but did not provide the correct pulse-height distribution.

3.4 Pulse height analysis

The pulse-height spectrum or pulse-height distribution can be defined as the variation of the magnitude of the output pulses when all controlled inputs are kept constant. Since the heights of the voltage pulses are proportional to the particles' associated energy, it is also referred to as the energy spectrum of the counter [13].

In this report, the term "pulse-height distribution" will be used not to confuse an amplitude distribution with a "frequency spectrum" (from a Fourier analysis that is used in signal processing). Figures 5a and 5b show the differential pulse-height distributions for thermal neutrons detected by ^{3}He and $^{10}BF_3$ counter tubes respectively [14].

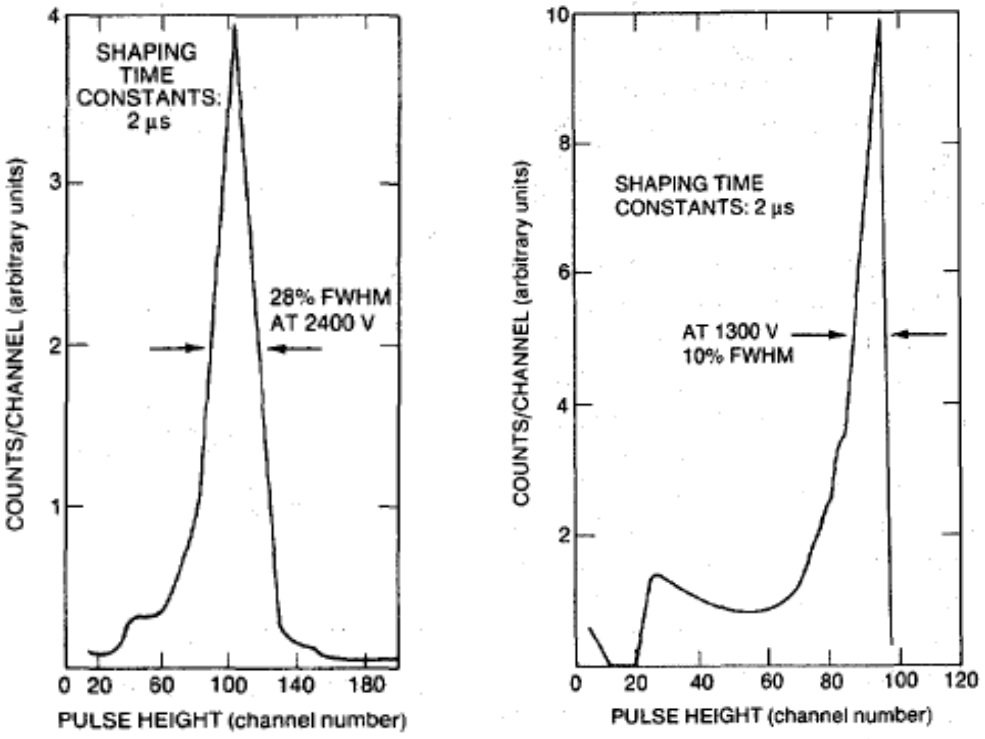

Figure 5a (left) and 5b (right): The differential pulse-height distribution for thermal neutrons detected by ^{3}He and $^{10}BF_3$ counter tubes respectively [14]

Similar distributions can be found in the datasheets of the counter tubes. These distributions indicate that the vast majority of pulses deposit a similar amount of charge on the detector wire. Furthermore, there is a clear distinction between the noise and the pulses created by neutron occurrences, which makes it easy for the noise to be cut out by setting a certain discrimination level.

The pulse-height distribution found in the datasheet [15] for the specific $^{10}BF_3$ counter tube used in the mini neutron monitor, which will also be used for testing the charge-sensitive amplifier, is given in Figure 6.

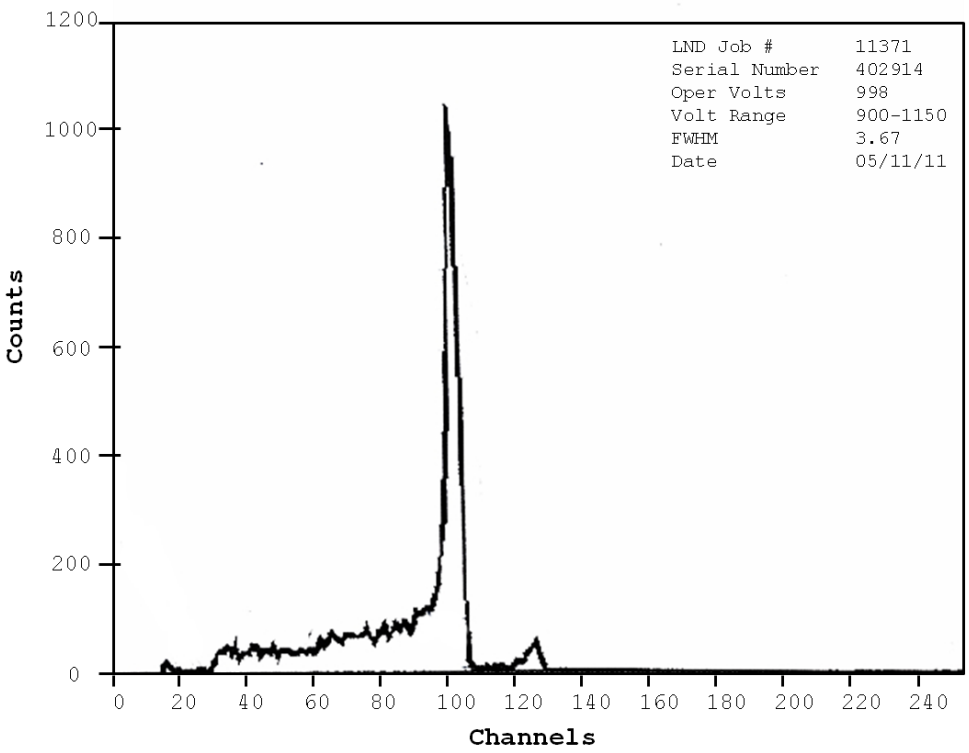

Figure 6: Pulse-height distribution for counter tube used in mini neutron monitor [15]

3.5 Amplifiers

Amplifiers are discussed – in general – to provide a background to physicists who will use the results of this research. Although this theory is familiar to the electronic engineering discipline, it is provided for the sake of completeness.

An amplifier is an electronic device to increase the amplitude of an electrical signal. The invention of the first amplifier came about with the invention of the three-element triode vacuum tube by Lee De Forest, the "Audion," in 1906. This was the first active device capable of signal amplification. De Forest added a control grid electrode, between the diode filament and plate, and an amplifier device was born [16].

While these first tubes of the 20th century had their drawbacks, the world of modern electronics was being born, and more key developments were soon to follow. The invention of the feedback amplifier principle at Bell Telephone Laboratories (Bell Labs) during the late 1920s and early 30s was truly an enabling development. This landmark invention led directly to the first phase of vacuum tube amplifiers, a general-purpose form of feedback amplifier using vacuum tubes, beginning in the very early 1940s and continuing through the World War II years [16].

After World War II, there was a transition period, as vacuum tube amplifiers were improved and refined, at least in circuit terms. These amplifiers were, however, fundamentally large, bulky, power-hungry devices. Vacuum tube amplifiers continued to flourish for some time into the 1950s and 1960s, but their competition was eventually to arrive from solid-state developments. These took the form of several key innovations, all of which required a presence before effective solid state operational amplifier designs could be established. There were three of these key developments, the invention of the transistor, the invention of the integrated circuit (IC), and the invention of the planar IC process [16].

A final major transitional phase of amplifier history began with the development of the first IC amplifiers, in the mid 1960s. Once IC technology became widely established, things moved quickly through the latter of the 20th century years, with milestone after milestone of progress being made in device performance [16].

3.5.1 Amplifier technology (general)

3.5.1.1 Transistor amplifiers

The transistor (a contraction for transfer resistor) is a multijunctional semiconductor device. Normally, the transistor is integrated with other circuit elements for voltage gain, current gain, or signal power gain. The bipolar transistor, also called the bipolar junction transistor (BJT), is one of the most important semiconductor devices [17].

BJTs have been used extensively in high speed circuits, analog circuits, and power applications. Bipolar devices are semiconductor devices in which both electrons and holes participate in the conduction process. This is not the same for field devices like the field-effect transistor (FET) in which predominantly only one kind of carrier participates [17].

The bipolar transistor was invented by a research team at Bell Laboratories in 1947. The device had two metal wires with sharp points making contact with a germanium substrate. The first transistor was primitive by today's standards, yet it revolutionised the electronics industry and changed our way of life [17].

The transistor is the heart of an amplifier. Bipolar transistors have traditionally been used in linear amplifier circuits because of their relatively high gain. Three basic single transistor amplifier configurations can be formed, depending on which of the three transistor terminals is used as signal ground. These three basic configurations are appropriately called common emitter, common collector (emitter follower), and common base. Which configuration of amplifier is used in a particular application depends to some extent on whether the input signal is a voltage or current and whether the desired output signal is a voltage or current [18].

Figure 7 shows the common emitter configuration [18]. The name common emitter comes from the fact that the emitter is common to both input and output, and is at ground potential for the sake of this discussion. The signal from the signal source is

coupled into the base of the transistor through the coupling capacitor C_C, which provides DC isolation between the amplifier and the signal source. The DC transistor biasing is established by R_1 and R_2, and is not disturbed when the signal source is capacitively coupled to the amplifier. There may be times when the emitter resistor must be large for the purposes of DC design, but degrades the small-signal voltage gain too severely. We can use an emitter bypass capacitor to effectively short out a portion or all of the emitter resistance as seen by the ac signals [18].

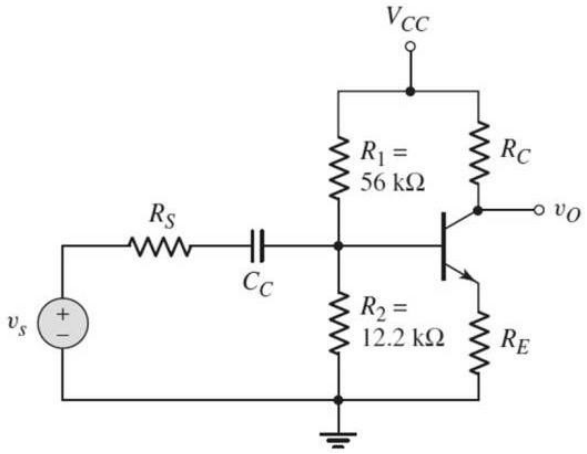

Figure 7: The common emitter transistor amplifier configuration [18]

The second type of transistor amplifier to be considered is the common-collector circuit. An example of this circuit configuration is shown in Figure 8 [18]. As seen in the figure, the output signal is taken off of the emitter with respect to ground and the collector is common to input and output and is connected directly to V_{CC} in this case. V_{CC} is at signal ground in the ac equivalent circuit. The more common name for this circuit is emitter follower [18].

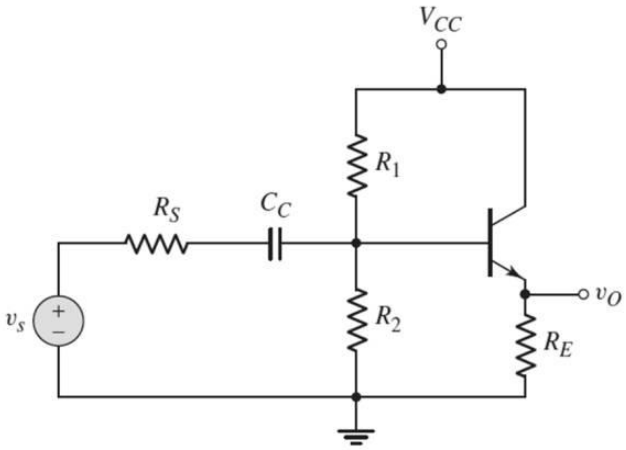

Figure 8: The common collector transistor amplifier configuration [18]

A third amplifier circuit configuration is the common-base circuit. Figure 9 shows the basic common-base circuit, in which the base is common (at signal ground) and the input signal is applied to the emitter [18].

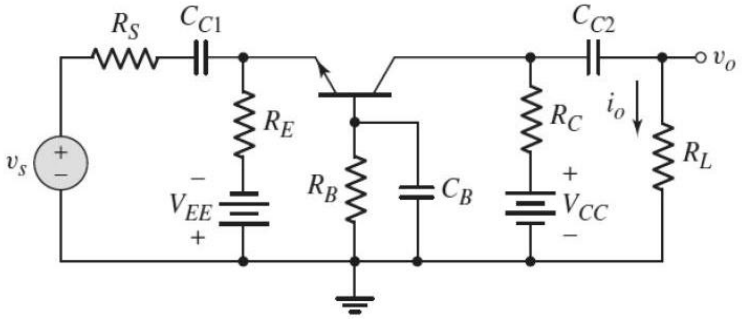

Figure 9: The common base transistor amplifier configuration [18]

The characteristics of these single-stage amplifiers can be used in the design of multistage amplifiers. In most applications, a single transistor amplifier will not be able to meet the combined specifications of a given amplification factor, input resistance, and output resistance. For example, the required voltage gain may exceed that which can be obtained in a single transistor circuit. Transistor amplifier circuits can be connected in series, or cascaded. This may be done either to increase the overall small-signal voltage gain or to provide an overall voltage gain greater than 1,

with a very low output resistance. The overall voltage or current gain, in general, is not simply the product of the individual amplification factors, and loading effects may have to be taken into account [18].

3.5.1.2 Operational amplifiers

An operational amplifier is an externally powered integrated circuit, made up of transistors, resistors, and capacitors, used to amplify an input signal.

The history of IC operational amplifier developments began with the work of Bob Widlar, back in the early 1960s. Starting with the first successful IC operational amplifier, the μA709, Widlar was to author virtually an unbroken string of IC operational amplifier successes [16].

The very first operational amplifiers were not even called such, nor were they even called "operational amplifiers". The naming of the device came after the war years, in 1947. It may be more clear to call one of these first operational amplifiers a general-purpose, DC-coupled, high gain, inverting feedback amplifier. This of course is a loose definition, but it nevertheless fits what transpired. A more detailed analysis for the name is given in the following six paragraphs [16].

General-purpose may be interpreted to mean that such an amplifier (or multiple amplifiers) operates on bipolar power supplies, with input and output signal ranges centred around 0 V (ground) [16].

DC-coupled response implies that the signals handled include steady-state or DC potentials, as well as AC signals [16].

High gain implies a magnitude of DC voltage gain in excess of 1000× (60 dB) or more, as may be sufficient to make system errors low when driving a rated load impedance [16].

Inverting mode operation means that this feedback amplifier had, in effect, one signal input node, with the signal return being understood as ground or common. Multiple signals were summed at this input through resistors, along with the feedback signal, via another resistor [16].

Note that this single-ended operating mode is a major distinction from today's differential input operational amplifiers. Operation of these first feedback amplifiers in only a single-ended mode was, in fact, destined to continue for many years before differential input operation became more widespread [16].

A *feedback* amplifier of this type could be used in a variety of ways, depending on the nature of the feedback element used with it. This capability of satisfying a variety of applications was later to give rise to the name [16].

An operational amplifier is designed to amplify the difference between the voltages applied to its two inputs with a very large amplification factor (A, open loop gain), typically 10^5 to 10^8. In addition, it provides very high input impedance and low output impedance, as is usually the case with preamplifiers. Negative feedback may be used in a variety of configurations to produce useful methods for manipulating analog signals [19].

The ideal operational amplifier possesses several unique characteristics. Since the device will be used as a gain block, the ideal amplifier should have infinite open-loop gain. By definition also, the gain block should have infinite input impedance in order not to add additional load to the signal source – that is, not to draw any power from the signal source. Additionally, the output impedance would be zero in order to supply infinite current to the load being driven [20].

3.5.1.3 Amplifier topologies

The term “instrumentation amplifier” is properly used to describe a category of true differential input amplifiers that emphasize high accuracy and amplifies the

differentiation of unwanted input signals (common to both input leads) relative to the wanted difference signal, also known as common-mode rejection (CMR) [21].

Although both instrumentation amplifiers and difference amplifiers use operational amplifiers as basic architectural building blocks, they are distinctly different from their operational amplifier cousins [21].

Operational amplifiers are single-ended and they are usually intended to operate in a variety of applications, with their feedback elements determining their functions. Instrumentation amplifiers and difference amplifiers are used primarily to provide differential gain and CMR. Employing feedback from output to input is not intended [21].

Most common instrumentation amplifiers are one of three types: the simple Difference Amplifier, the Classical Three-Operational Amplifier Instrumentation Amplifier, and the Two-Operational Amplifier Instrumentation Amplifier architecture [21].

The simplest form of instrumentation amplifier is the Difference Amplifier, an operational amplifier with four precision resistors as shown in Figure 10 [21].

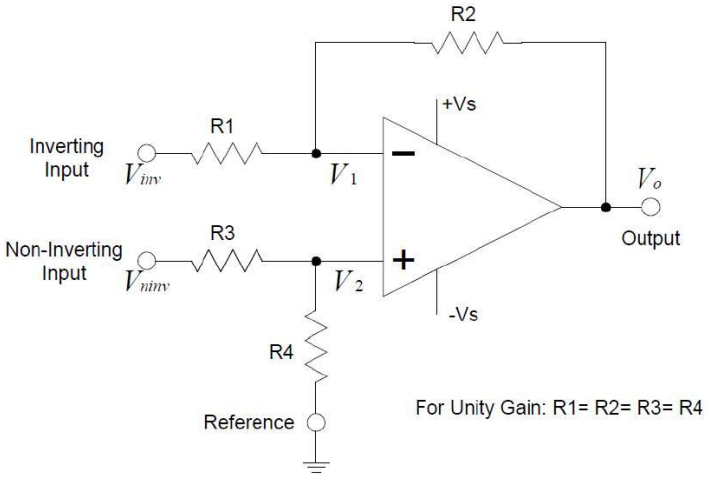

Figure 10: The unity gain difference amplifier [21]

The simple single operational amplifier differential amplifiers have one outstanding disadvantage over the two and three-operational amplifier configuration instrumentation amplifiers: low input impedance. A finite input impedance will cause the amplifier to draw current from the signal source, leading to the loading effecet whereby the signal delivered to the amplifier is smaller. This low input resistance, coupled with the severe limitation of requiring equal source resistances to prevent CMR degradation, makes the two and three-operational amplifier instrumentation amplifier more attractive than the difference amplifier in many applications [21].

Since the limitations of the difference amplifier are input-resistance related, a buffer amplifier can be put on the inputs to solve these problems. Not only will this resolve the difference amplifier limitations and achieve very high input impedance, these input buffer amplifiers can also provide voltage gain. An example is shown in Figure 11 [21].

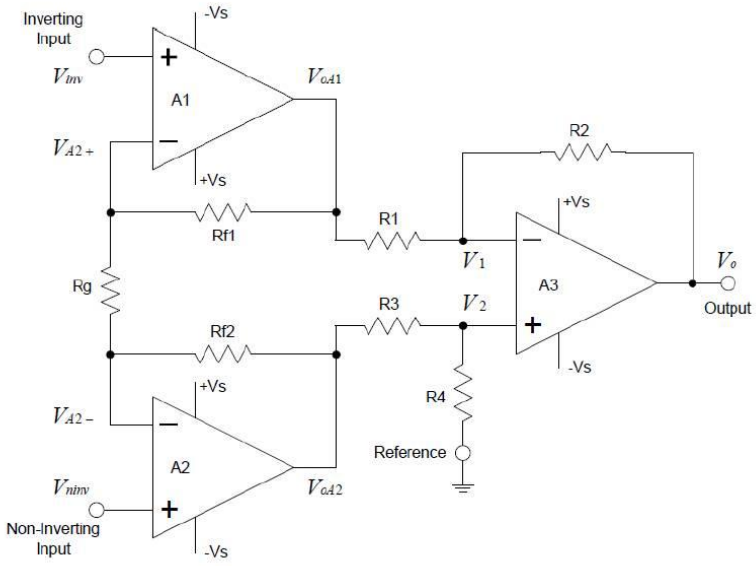

Figure 11: The Three-operational amplifier instrumentation amplifier [21]

Operational amplifiers A_1, A_2, and the feedback network R_g, R_{f1}, and R_{f2} form a differential input, differential output amplifier that drives an output stage difference

amplifier (A_3 plus R_1, R_2, R_3, and R_4). The output difference amplifier function in the three-operational amplifier instrumentation amplifier is to provide CMR [21].

The input amplifiers may provide gain but no CMR. CMR is provided solely by the output difference amplifier. As amplifiers A_1 and A_2 are non-inverting operational amplifiers, the input impedance is very high, thus eliminating any undesirable source loading and removing the strict requirement of having equal source impedances at each input. In fact, except for having to consider input bias current effects, the instrumentation amplifier's inputs do not affect the signal source at all [21].

To reduce the size of the silicon substrate used in the amplifier's IC, and thus reduce manufacturing cost, a simpler, two-operational amplifier instrumentation amplifier can be used that still has an input impedance as high as that of the three-operational amplifier instrumentation amplifier. The only sacrifice that is made is that unity gain is no longer possible. An example is shown in Figure 12 [21].

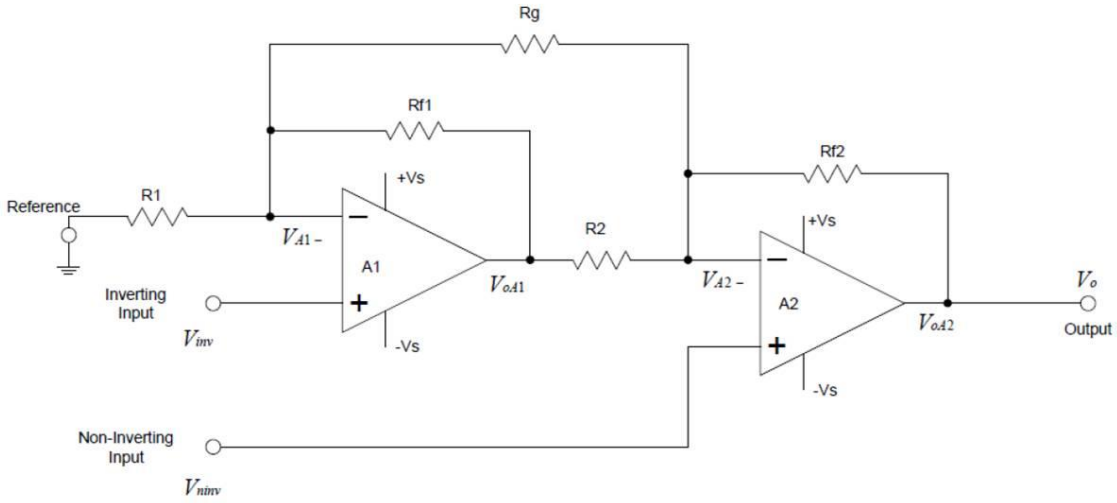

Figure 12: The Two-operational amplifier instrumentation amplifier [21]

Because of differences in the noise gain of the two operational amplifiers, the two-operational amplifier instrumentation amplifier does not preserve symmetry of its common mode error well at higher frequencies and, as a result, its CMR falls off

faster with frequency than a classical three-operational amplifier circuit. Due to the equal noise gains of the two input operational amplifiers in a three-operational amplifier instrumentation amplifier, their bandwidths are well matched and there is little unmatched “residual error” to degrade CMR at high frequencies [21].

The two basic feedback topologies used are voltage feedback and current feedback, shown in Figures 13 and Figure 14 respectively [16].

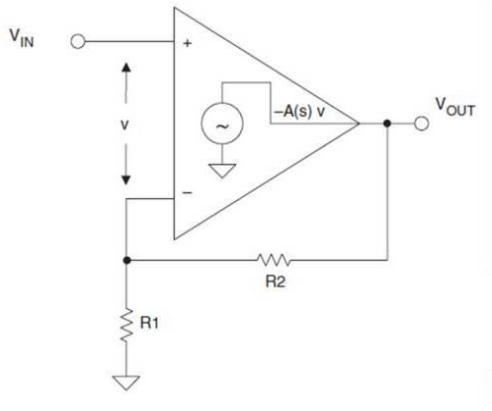

Figure 13: Voltage feedback operational amplifier topology [16]

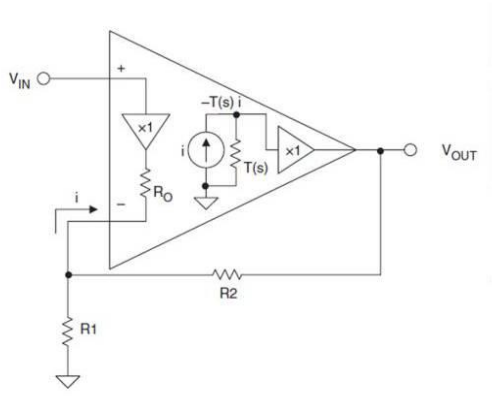

Figure 14: Current feedback operational amplifier topology [16]

These two types of amplifiers are distinguished more by the nature of their internal circuit topologies that anything else. The voltage feedback operational amplifier

topology is the classic structure and includes most operational amplifier models produced today [16].

Within the model for the current feedback amplifier topology, a unity gain buffer connects the non-inverting input to the inverting input. In the ideal case, the output impedance of this buffer is zero, and the error signal is a small current which flows into the inverting input. The error current is mirrored into a high impedance. This voltage is then buffered and is connected to the operational amplifier output [16].

3.5.1.4 Operational amplifier noise vs. transistor noise

In electrical circuits there are five common noise sources [22]:

- Shot noise;
- Thermal noise;
- Flicker noise;
- Burst noise;
- Avalanche noise.

Shot noise is always associated with current flow. It results whenever charges cross a potential barrier, like a P-N junction. Crossing the potential barrier is a purely random event. Thus the instantaneous current is composed of a large number of random, independent current pulses with an average value. It is generally specified in terms of its mean-square variation about the average value. Shot noise is spectrally flat or has a uniform power density, meaning that when graphed over a frequency range, it has a constant value. Shot noise is independent of temperature [22].

Thermal noise is caused by the thermal agitation of charge carriers (electrons or holes) in a conductor. This noise is present in all passive resistive elements. Like shot noise, thermal noise is spectrally flat or has a uniform power density, but thermal noise is independent of current flow. Thermal noise in a conductor can be modeled as voltage or current. When modeled as a voltage it is placed in series with an

otherwise noiseless resistor to form a Thévenin voltage source. When modeled as a current it is placed in parallel with an otherwise noiseless resistor to form a Norton current source [22].

Flicker noise is also called 1/f noise. It is present in all active devices and has various origins. It is always associated with a DC current. Flicker noise is also found in carbon composition resistors where it is often referred to as excess noise because it appears in addition to the thermal noise. Other types of resistors also exhibit flicker noise to varying degrees, with wire-wound showing the least. Since flicker noise is proportional to the DC current in the device, then if the current is kept low enough, thermal noise will predominate and the type of resistor used will not change the noise in the circuit [22].

Burst noise, also called “popcorn” noise, appears to be related to imperfections in semiconductor material and heavy ion implants. Burst noise makes a popping sound at rates below 100 Hz when played through a speaker. Low burst noise is achieved by using clean device processing so as to prevent impurities in the semiconductor material [22].

Avalanche noise is created when a PN junction is operated in the reverse breakdown mode. Under the influence of a strong reverse electric field within the junction’s depletion region, electrons have enough kinetic energy that, when they collide with the atoms of the crystal lattice, additional electron-hole pairs are formed. These collisions are purely random and produce random current pulses similar to shot noise, but much more intense [22].

In operational amplifier circuits, burst noise and avalanche noise are normally not problematic, or they can be eliminated if present [22]. There are two noise sources in an operational amplifier that are of concern, namely (i) voltage noise, which appears differentially across the two inputs and (ii) current noise in each input. These sources are effectively uncorrelated. In fact, there is a slight correlation between the two

noise currents, but it is too small to warrant consideration in practical noise analyses. The voltage noise of different operational amplifiers may vary from under 1 nV/√Hz to 20 nV/√Hz, or more. Voltage noise is specified on the specific amplifier data sheet, and it is not possible to predict it from other parameters [23].

Current noise can vary much more widely, from around 0.1 fA/√Hz to several pA/√Hz. It is not always specified on data sheets, but may be calculated in cases where all the bias current flows in the input junction, because in these cases it is simply the shot noise of the bias current. It cannot be calculated for bias-compensated or current-feedback operational amplifiers, where the external bias current is the difference of two internal current sources [23].

Current noise is only important when it flows in an impedance and generates a noise voltage. Therefore, the choice of a low-noise operational amplifier depends on the impedances around it. With zero source impedance, voltage noise will dominate. With a source resistance of a few hundred kΩ, the current noise increases significantly, while the voltage noise remains unchanged, therefore, current noise is dominant [23].

Uncorrelated noise voltages add in a “root-sum-of-squares” manner, while noise powers (in essence, variances) add algebraically. Thus, any noise voltage that is more than 3 to 5 times any of the others is dominant, and the others may generally be ignored. This simplifies noise assessment [23].

The primary noise sources in field-effect transistors are thermal noise in the channel and gate current. Since the area of the gate is small, this contribution to the noise is very small and usually can be neglected. Thermal velocity fluctuations of the charge carriers in the channel superimpose a noise current on the output current. In a FET the gate noise current is the shot noise associated with the reverse bias current of the gate-channel diode [24].

Voltage noise tends to originate within a device (e.g. thermal noise of a FET channel or collector shot noise in a BJT) and appears as a noise current at the output, which is mathematically transformed to the input. This noise voltage is not physically present at the input and is not affected by any connections or components in the input circuit [24].

The noise voltage sources that represent all voltage noise contributions of a given amplifier are in series with the individual inputs. Since the input impedance of the amplifier is effectively infinite, the source impedance is by definition negligible in comparison, so the noise voltage associated with a given amplifier only develops across the input of that amplifier [24].

The noise characteristics of bipolar transistors differ from field-effect transistors in four important aspects [24]:

- The equivalent input noise current cannot be neglected, due to base current flow;
- The total noise does not decrease with increasing device current;
- The minimum obtainable noise does not depend on the shaping time;
- The input capacitance is usually negligible.

Since the base current noise increases with shaping time, bipolar transistors are only advantageous at short shaping times. With current technologies, FETs are best at shaping times greater than 50 to 100 ns, but decreasing feature size of MOSFETs will improve their performance. For the transimpedance case, FET amplifiers are a better choice as they generally have much lower input current noise than BJTs [24].

For a low source resistance, a low-noise bipolar transistor works well and provides high gain. For a high source resistance, a low noise field-effect transistor is more suitable. Noise current at the input of a FET is a fraction of that for a bipolar

transistor and even at high impedances the equivalent noise voltage generator is the dominant factor [25].

Discrete bipolar transistors running at very low collector currents demonstrate a lower noise voltage than operational amplifiers. Low equivalent noise is better achieved using discrete transistors with controlled collector (or drain) current rather than integrated circuit packages [25].

3.5.2 Charge-sensitive amplifiers

Charge-sensitive amplifiers take an input current pulse and deliver an output voltage proportional to the total charge contained in the input pulse [26]. A charge-sensitive amplifier is thus a current integrator of capacitive nature.

The basic circuit diagram for a charge-sensitive amplifier, or what is also referred to as an *integrating amplifier*, is shown in Figure 15 [26].

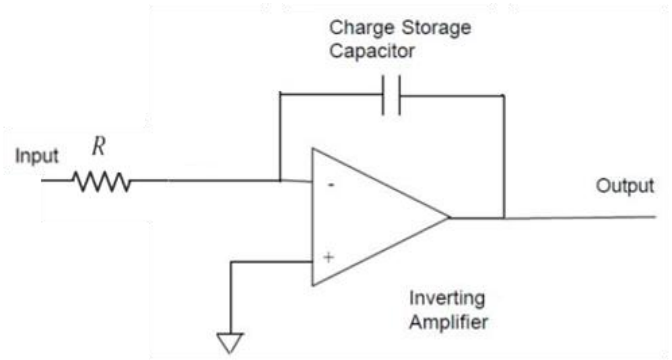

Figure 15: Circuit diagram for a basic charge-sensitive amplifier [26]

The voltage across the initially uncharged storage capacitor is given by the following expression:

$$v = \frac{1}{C}\int_0^{t_1} idt\,, \tag{1}$$

where *i* is the current through *C*, and t_1 is the integration time [27].

For the integrator, and for v_{in} positive, the input current flows through *C* in a direction to cause v_{out} to move in a negative direction. Thus the following expression is obtained:

$$v_{out} = -\frac{1}{RC}\int_0^{t_1} v_{in}dt + v_{init} \quad , \tag{2}$$

where *R* is an input resistance (if applicable) and v_{init} is the voltage due to the initial condition [27].

This shows that v_{out} is equal to the negative integral of v_{in}, scaled by a factor determined by the input circuitry and added to the voltage due to the initial condition [27].

This performs two useful functions, namely: (i) the integration performed by the amplifier serves to filter high-frequency noise, and (ii) the output pulse can be many times longer than the input pulse. A further advantage of a charge-sensitive amplifier is that all output pulses have the same shape and decay time constant, assuming that the input pulse is much shorter than the decay time constant. This makes subsequent pulse processing much easier [26].

The major circuit elements of a charge-sensitive amplifier are: an inverting amplifier; a feedback charge storage capacitor; and a reset circuit. The capacitor stores charge from input pulses so that a voltage appears on the output proportional to the total charge in the input pulse. The reset network discharges the capacitor between pulses. Without the reset circuit, the output voltage is essentially a step function,

with an extremely long decay time dependent on the amplifier offset voltage, input bias current, and miscellaneous leakage currents [26].

The removal of the input charges from the feedback capacitor can be realised either periodically by a clock controlled switch, or by a parallel feedback resistor, R_f. Since the arrival of the particles occurs at random, a continuous reset is needed, and a feedback resistor is employed to set the voltage across the capacitor to its initial value [28].

A representation of the charge-sensitive amplifier with reset circuit is shown in Figure 16 [26].

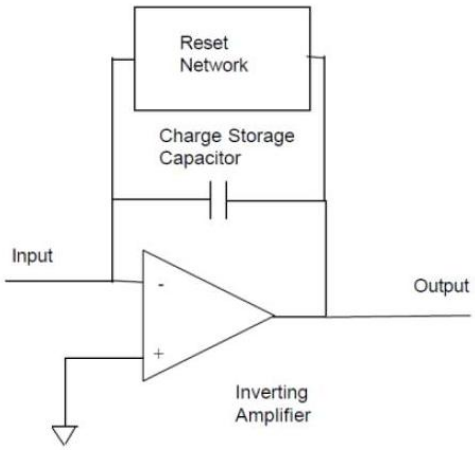

Figure 16: Basic implementation of a charge-sensitive amplifier [26]

Each neutron occurrence causes a specified amount of charge on the counter tube anode (wire). This charge can be generated at a high flow rate, causing the output pulse to have a very steep rising slope, or it can be provided slowly, causing a reduction in the slope angle. For both the fast or slow occurrences, the amount of charge deposited on the wire is the same, which means that the area under the two curves should be equal. In order to obtain the correct pulse-height distribution, we need to measure the area under each pulse instead of the actual pulse height.

The conversion of charge, *Q*, into a measurement voltage involves, at some stage, the transfer of that charge into a reference capacitor (also known as the feedback capacitor), C_f. The voltage V_r developed across the capacitor gives a measure of the charge as $Q = \frac{V_r}{C_f}$ [29].

The characteristics of such amplifiers include the following [19]:

- High gain
- Low noise
- Integration linearity
- Short rise time
- High temperature stability
- Long RC discharge time
- No charge leakage

3.5.2.1 Charge Amplifier Gain

The gain of the charge amplifier can be considered in one of two ways, namely: the gain for the amplifier; or the gain for a detector/amplifier combination. The gain of the amplifier, also referred to as *charge gain* is given by the following expression [30]:

$$G_c = \frac{V_{out}}{Q_s} = \frac{1}{C_f} \tag{3}$$

In this case the term *sensitivity* is generally used, rather than gain. Sensitivity is expressed as the output voltage (mV) per one MeV of particle energy irradiated onto a detector [30].

3.5.2.2 Charge Amplifier Noise

Noise in neutron detector systems using charge-sensitive preamplifiers has been the subject of many publications [31] - [35]. As in most applications, noise can be referred to equivalent input noise sources, or equivalent noise charge (ENC) [36].

It is common in amplifier noise modeling to refer all circuit noise sources back to the inputs using equivalent input noise sources. This can be done as the noise of the first stage in a high-gain circuit contributes the most to the overall circuit noise, as is well known from the analysis of cascaded amplifiers. The equivalent input noise is given in terms of a voltage noise density (V/√Hz) and a current noise density (A/√Hz) [36].

The charge-sensitive amplifier is characterised by a series input voltage noise source, e_n, with a white-noise component set by the input device transconductance, g_m, as well as a 1/f component that is inversely proportional to the device area. In many cases the equivalent input noise current is negligible, but the secondary feedback element R_f, which discharges the feedback capacitor, contributes noise whose impact must be carefully considered [37].

Typically, series white noise dominates for short shaping times, R_p for long shaping times, and 1/f noise in the intermediate range. High capacitance detectors intensify the series noise terms. While both series white noise and parallel noise can be decreased by amongst others, circuit techniques and expenditure of more power, the effect of 1/f noise on charge-sensitive amplifier performance is fundamentally limiting [37].

3.5.2.3 Charge-sensitive amplifier application study

When doing research on the applications and implementations of charge-sensitive amplifiers, many sources [28], [38] - [40] can be located where they were successfully used in systems such as X-ray or gamma detection, as well as in radiation detection applications where the radiation is detected in a series of pulses, as is also the case

for this application. Companies like Cremat [41], Amptek [42], and Ortec [43] manufacture various charge-sensitive amplifiers for implementation with different particle detectors. *These amplifiers are, however, costly and not readily available.* They are also not well-suited for all applications, and with some systems, interface circuitry still has to be used to effectively connect the amplifier to the detector and/or following systems. After consultation with the parties that will benefit from this project, considering input received from an expert in amplifier design for neutron monitors [44], it was decided that designing a preamplifier to meet the specific needs of the neutron monitor used at the Centre for Space Research at the North-West University would be the most effective solution. This would allow for a design from first principles using transistors and basic passive circuit components to deliver an amplifier where the custom parameters of the new neutron monitor design will be best catered for. This solution would also be cost effective and due to the design choices, will ensure availability.

Information from the existing literature on these applications can be used to aid in the synthesis and design of a charge-sensitive amplifier specifically for the new neutron monitor system being constructed by the Centre for Space Research at the North-West University.

There are a number of considerations and trade-offs to make when choosing the correct charge-sensitive preamplifier for an application [45]. From the Cremat application notes [45], the following valuable guidelines were obtained, as discussed below.

1) Maximum detectable pulse

In choosing a preamplifier for an application, it is often best to start by considering the model that has the highest gain. A potential problem, however, is that too much gain will cause larger signal pulses (larger than approximately 10^7 electrons) to

saturate the preamplifier circuitry. In such applications it is best to choose a less sensitive preamplifier [45].

A good approach to selecting the right preamplifier is to choose the model that has the largest gain which is also capable of detecting the largest pulses the designer expects to detect in their applications [45].

2) Stability at high input capacitance

In applications where the input capacitance to the preamplifier exceeds 2000 pF, some preamplifiers become unstable and may oscillate. In these rare applications designers should select a preamplifier model which is stable at a high input capacitance [45].

3) Rise-time performance

The rise-time performance of charge-sensitive preamplifiers varies amongst various models, and also depends on the capacitance at the preamplifier input. Keep in mind that in some detectors, rise time will be limited by the detector itself. In these cases the use of a faster preamplifier will not improve the situation. In applications with fast detectors, however, the designer may wish to choose a preamplifier with these preamplifier rise time specifications taken into consideration [45].

4) High count rate

In high count rate applications, the preamplifier circuitry can sometimes saturate due to the high rate of detector current being sourced or sunk at the preamplifier input. In these high-rate applications, the designer may wish to avoid the high gain preamplifier models which are the most prone to this saturation [45].

Calculating whether a particular preamplifier can process a certain count rate is complicated, because the answer depends on the distribution of pulse sizes being detected and the distribution of events over time (e.g. random over time, occurring

only during certain time windows, etc). A somewhat simplified approach would be to assume that the pulses occur totally randomly over time and that the detected pulses are a large amount of small pulses (rather than a few number of larger sized pulses) [45].

If one assumes that the preamplifiers are DC coupled to the detector, then it is possible to treat the simplified detector current described above as a DC current passing into the preamplifier input. In this simplified case, the maximum count rate the preamplifier would be able to process would be that which produced a detector current equal to the maximum DC input current. Note that usually the high gain preamplifiers have the worst count rate processing ability. Also consider that the assumption that the detector current is comprised of many small pulses represents a best-case condition for the preamplifier maximum count rate [45].

If AC coupling is used between the detector and preamplifier, the count rate capability of the preamplifier is dramatically increased, at least if one uses the simplifying assumption that the detector signal current is made up of many small pulses. Using AC coupling, the DC detector current no longer passes into the preamplifier input. As a result, the preamplifier output saturates only when the output *fluctuations* become so large that they exceed the rail-to-rail output range of the preamplifier. The size of these fluctuations depends on the size distribution and rate of the detected pulses, and it is difficult to quantitatively describe the count rate limitations of the preamplifiers under these conditions. It remains true, however, that the highest gain preamplifiers generally have the worst count rate processing ability and the lowest gain have the best count rate processing ability [45].

An article from the Radiation Physics and Chemistry journal application notes [46], noted the following:

"In this journal article, the use of commercial operational amplifiers in a low cost multi-channel preamplifier system that can be used as a suitable operational amplifier for the preamplifier stage of radiation detectors is described."

Although various IC operational amplifiers are commercially available, there are only a few operational amplifiers which can be used for radiation charge-sensitive preamplifiers. The basic properties of suitable operational amplifiers are briefly described in the following [46]:

1) Input noise

A major limitation on the choice of operational amplifiers is input noise. The noise current flows through the source impedance (Z_s) resulting in a noise voltage i_nZ_s. This is added to the equivalent input noise voltage e_n, resulting in the total equivalent input noise voltage:

$$e_n^{tot} = \sqrt{e_n^2 + (i_n Z_s)^2} \quad (4)$$

The operational amplifiers with FETs as the input stage exhibit a low equivalent noise due to their extremely low equivalent input noise current, which makes them potentially a good choice for charge-sensitive preamplifiers [46].

2) Open loop gain

The open loop gain should be large to ensure that all the charge goes to the feedback capacitor and also to ensure that the preamplifier sensitivity is unaffected by external capacitance changes due to detector or input cabling. An open loop gain of greater than 50dB is usually required to satisfy these conditions [46].

3) Input bias current

A major determinant of the performance of the preamplifier is the input bias current of the operational amplifiers. A low input bias current is required not only for minimization of output DC error, but also for a proper setting of the feedback resistor (R_f). Since the DC path to the input bias current of the operational amplifiers is provided by the resistor feedback, the resistor value should be chosen in accordance with the input bias current. A large input bias current limits the feedback resistor value, while the value of feedback resistor should be small enough to minimize the resistor thermal noise and also provide a sufficient preamplifier time constant (R_fC_f) for a full charge collection inside the detector. Consequently, for a proper setting of the feedback resistor, operational amplifiers with input bias currents in the order of a few pico Amperes are desirable [46].

4) Bandwidth and slew rate

A large bandwidth is required in order to avoid distortion in the shape of signals and to maintain preamplifier stability and low noise through a proper setting of the feedback values, particularly for detectors with large capacitance. In high rate applications, like imaging systems, the ideal amplifier should also have a large slew rate so that no distortion of the pulse shape would occur at high pulse processing rates. High bandwidth is however a trade-off to gain and higher equivalent input noise [46].

Although the noise performance of the preamplifier discussed in this journal is slightly larger than the noise of commercial preamplifiers, the energy resolution is sufficient for the application discussed. The power consumption of this preamplifier is rather high, which might be a concern for some applications [46].

The concept of using a diode as feedback circuitry is discussed in the Nuclear Instruments and Methods in Physics Research A journal for use in a logarithmic amplifier used as part of the front-end electronics for a $^{10}BF_3$ neutron monitor. Using a diode instead of a conventional capacitor in a circuit ensures a lower tolerance level since the manufacturing process of a diode is more controlled than that of a capacitor of similar value, at a fraction of the cost of a low tolerance capacitor [47].

The most important properties of a charge-sensitive amplifier that needs to be addressed in the synthesis and design process are negligible input and output impedance for optimum coupling with the generating or detecting element and the subsequent electronics, high sensitivity, and low noise to increase the signal to noise ratio (SNR) [48].

3.6 Synthesis from the literature study

In order to follow a DSR approach in this research, a theoretical problem and problem statement was defined. This theoretical problem was then investigated by doing an extensive literature study on the subject matter in order to assist in the synthesis and design choices of the artefact that would solve the real-world problem.

The literature study revealed the method of operation of a neutron monitor [6] - [12], as well as the correct shape of a pulse-height distribution graph for proportional counter tubes [13] - [15]. This also set the standard against which the designed amplifier's pulse-height distribution would be measured.

A study was done on different amplifiers [16] - [20] and amplifier configurations or topologies [18], [21]. This showed that operational amplifiers posses several unique characteristics such as very high input impedances in order not to add additional load to the signal source, as well as very low output impedances in order to supply (theoretically) infinite current to the load being driven. The study also showed that, by using discrete transistor amplifiers, a high level of flexibility is obtained. The

characteristics of these single-stage transistor amplifiers can be used in the design of multistage amplifiers by means of cascading to cater for specific requirements.

When the noise of operational amplifiers and transistor amplifiers was considered [22] - [25], it was noted that although other types of noise are present, flicker noise, or 1/f noise, is generally the most dominant in amplifiers operating in the intermediate shaping time range. It was seen that discrete bipolar transistors running at very low collector currents produce a lower noise voltage than operational amplifiers. Low equivalent noise is better achieved using discrete transistors with controlled collector (or drain) current rather than integrated circuit packages. Noise current at the input of a FET is a fraction of that for a bipolar transistor and even at high impedances the equivalent noise voltage generator is the dominant factor.

From this information, the design choice was made to use a discrete transistor amplifier with a FET buffer stage as the first stage. This would ensure a higher level of flexibility in the design as well as low noise.

A study of charge-sensitive amplifiers [19], [26] - [29] showed that this type of amplifier takes an input current pulse and delivers an output voltage proportional to the total charge contained in the input pulse. All output pulses have the same shape and decay time constant, which would provide the desired pulse-height distribution graph. The major circuit elements of a charge-sensitive amplifier are an inverting amplifier, a feedback charge storage capacitor and a reset circuit. The reset circuit can either be a clock-controlled switch, or a large valued resistor. For random events, a continuous discharge, or resistor, feedback is required. From this information, the design choice was made to synthesise a charge-sensitive amplifier with a large valued resistor as reset circuit.

From the application study of charge-sensitive amplifiers [28], [38] - [46], it was recommended that during the synthesis and design process, considerations should be made for the following:

- Maximum detectable pulse;
- Stability at high amplifier input capacitance;
- Rise-time and decay-time performance;
- Acceptable count rate;
- Input noise;
- Open loop gain;
- Input bias current;
- Bandwidth and slew rate.

The most important technical properties of the amplifier that the synthesis and design process should address are: (i) high input and low output impedance for interfacing, (ii) high sensitivity, and (iii) low noise [48]. As availability, cost and flexibility also played an important role, it was decided to use readily available discrete components (with a MOSFET transistor at the core of the design) to address these considerations.

3.7 Summary

In this chapter, an overview of existing literature on neutron monitors, pulse-height distributions of proportional counter tubes, amplifiers (in general) and charge-sensitive amplifiers was presented.

It was mentioned that neutron monitors have been in use since the 1950s, and even though the monitors used by the Centre for Space Research at the North-West University were redesigned in 2003, the electronic subsystem has become outdated and needs to be replaced. It was decided that the new design will employ a microprocessor to register and count pulses from counter tubes.

After doing an investigation on the current preamplifiers used in the North-West University's neutron monitor, it was observed that these preamplifiers deliver an incorrect pulse-height distribution graph. The correct shape for this graph can be found in the datasheet for the specific counter tube used. These distributions indicate that the vast majority of pulses deposit a similar amount of charge on the detector wire.

An investigation was done on amplifier topologies and their characteristics. From this it was seen that a charge-sensitive amplifier would amplify the charge deposited on the counter tube wire by each neutron occurrence rather than amplifying only the peak pulse height. This would result in the desired pulse-height distribution graph shape.

A comparison between the noise in transistor amplifiers and operational amplifiers was done and showed that the primary noise sources in operational amplifiers are flicker, thermal, and shot noise, and in field-effect transistors thermal noise in the channel and gate currents are present. It was seen that discrete bipolar transistors running at very low collector currents demonstrate a lower noise voltage than operational amplifiers. Noise current at the input of a FET is a fraction of that for a bipolar transistor and even at high impedances the equivalent noise voltage generator is the dominant factor.

It was seen that charge-sensitive amplifiers have a feedback charge storage capacitor and a reset circuit, which is usually a large valued resistor. An input current pulse is measured, and an output voltage proportional to the total charge contained in the input pulse is delivered. Not only does this make subsequent pulse processing much easier, but the integration performed by the amplifier serves to filter high-frequency noise, and the output pulse can be significantly longer than the input pulse.

It was observed that with charge-sensitive amplifiers, all output pulses would have the same shape and decay time constant, confirming that this type of amplifier would

be an ideal candidate to use in the neutron monitor system in order to obtain the specified pulse-height distribution curve.

From the literature on different applications of charge-sensitive amplifiers, it was noticed that even though preamplifiers for use in particle detection systems can be bought as an off-the-shelf module, these amplifiers are costly and not always effective for custom applications.

For the purpose of cost-effectiveness, availability, optimum coupling with the detector and subsequent circuitry, and parameters that can be adjusted to suit the specific needs of the application, benefactors of this project have approved the design of a custom-designed, discrete, charge-sensitive preamplifier that will cater for the specific parameters of the new mini neutron monitor being constructed at the North-West University.

4. Synthesis and experimentation

This chapter details the synthesis of the charge-sensitive amplifier using the literature survey found in the previous chapter, as well as simulation experiments.

4.1 Introduction

As the amplifier will be used in a real-world application, it is imperative to show that the design in this design science research process addresses requirements as obtained from an analysis of the real-world problem. That is, the amplifier must address the derived requirements as obtained by analysing the neutron monitor system. It is important to note that by addressing the real-world requirements, the *charge-sensitive amplifier artefact is validated*.

Simulations formed part of the design process and were used to provide an amplifier topology that is used to physically construct a charge-sensitive amplifier.

The chapter layout is as follows: A requirements analysis of the real-world problem is presented; the simulation design along with the results of different simulation tests is then presented; and finally the design of the amplifier, as it will be manufactured, is shown.

4.2 Requirements for the real-world artefact

The requirements that the real-world artefact must meet are described in the sections that follow. In all instances, the design approach and evaluation are given to show how requirements will be addressed and evaluated.

4.2.1 Pulse amplification

Pulse amplification requirements – the preamplifier must amplify charge, with the voltage output of the preamplifier proportional to the total charge on the proportional tube's detector wire. The total integrated charge will typically be 3.3 pC as determined from measurements at the Centre for Space Research. The gain of the preamplifier must be constant for different pulse durations and constant total charge. External gain will be added afterwards to provide a voltage that can be accurately digitized by a microcontroller (the external gain element was not part of the scope of this research).

Thus, the output voltage of the preamplifier will be directly proportional to the charge of each event pulse, which is in turn directly proportional to the energy each particle delivers to the counter tube. The pulse shape must be representative of the pulse shape as obtained from the neutron counter tube data sheet. The output pulse shape should thus be representative of a pulse shape as obtained from an integrating amplifier.

4.2.2 Electrical interface

The input impedance of the preamplifier must meet the counter tube interface requirements so as not to load the counter tube. This is a design requirement that will be addressed by means of component selection.

The output voltage must be 35 mV ± 2mV for an input of 3.3 pC as for the existing preamplifier and counter tubes used. The shaping amplifiers that follow the preamplifier are calibrated during manufacturing. Hence, the output voltage of the preamplifier is not critical in terms of its accuracy. The gain should thus be approximately 35 mV / 3.3 pC ≈ 10.6 mV / pC.

4.2.3 Power supply interface

The preamplifier must operate from the existing power supply for legacy reasons. The power consumption was not specified, but a low-noise amplifier's current is usually limited to low values. In this case, the consumption is specified to be less than 10 mA.

4.2.4 Noise

A low-noise design must be delivered to ensure acceptable noise performance. This is a design requirement and an appropriate low-noise configuration must be selected from literature, with sufficient evidence that the selection is acceptable. The evidence will be provided in the form of simulations, as PSpice is considered to be accurate in simulating noise generated by physical components (an advantage of using physical components in simulations as opposed to ideal components).

Protection against external interferers will be provided by using the existing EMI shield. This EMI shield is part of a previous project and falls outside the scope of this work. However, the shield had been functioning previously and will be used as provided.

4.2.5 Linearity

The preamplifier must be linear inside the operating region. This is a design requirement that must be met as non-linearity will result in an incorrect pulse-height distribution. This requirement requires that the input charge be adjusted while the output is determined. Amplifier gain for different pulse durations will be evaluated, which is equivalent to increasing the total charge on the input – the amplifier must remain linear for a total charge of 3.3 pC and input pulses between 1 µs and 10 µs. Simulations and measurements will be used to evaluate linearity.

4.2.6 Rise and decay time

Typical rise and fall times must be provided so that the preamplifier operates under realistic input conditions. The input pulse will have a rise time of no less than 1 µs and a decay time of no longer than 300 ms, with a total pulse charge of 3.3 pC. As a result, simulations will be run for input pulses with a minimum rise time of 1 µs and maximum fall time of 4 µs with amplitude selected so that the total charge will be 3.3 pC. Three pulses were selected, namely:

- Pulse 1: Peak input current of 2.2 µA, and rise and fall times of 1 µs and 2 µs respectively;
- Pulse 2: Peak input current of 1.32 µA, and rise and fall times of 2 µs and 3 µs respectively;
- Pulse 3: Peak input current of 0.943 µA, and rise and fall times of 3 µs and 4 µs respectively.

4.2.7 Temperature

The preamplifier must exhibit acceptable temperature characteristics for use in a controlled neutron monitor environment. That is, an operating range of 25 °C ± 10 °C is required. As the neutron counter measures temperature and can provide temperature correction, it is not a requirement to provide constant gain across the temperature range, but rather to provide the characteristics of the preamplifier across the required range. Simulations will show whether the temperature variation is excessive inside the operating region. Temperature simulation in PSpice is also known to be reliable and the results from simulations will be considered sufficient. In order to evaluate the artefact at temperatures outside the specified region, simulations shall be run at temperatures between -10 °C and 50 °C.

4.2.8 Physical form factor

In order to interface to existing sub-systems such as the counter tube and counting circuitry, the physical form factor must match the existing form factor. This requirement is addressed by means of physical design. Inspection will show whether this requirement was successfully addressed.

4.2.9 Cost and availability

It is imperative that a solution must be provided using components that are available and affordable. No special purpose devices should be used as the preamplifier will be in service globally and long procurement lead times and unavailability constraints are not acceptable. Cost and availability will be addressed by slelcting readily available components.

4.3 Simulation design

After consulting existing literature on the synthesis and applications of charge-sensitive amplifiers [28], [38] - [41], [46], [48], as well as the design support of an expert in amplifier design for neutron monitors [44], a basic configuration for the amplifier was selected. Because of the custom application, as well as the need for specific parameters, the amplifier will be using a transistor design instead of an integrated circuit operational amplifiers or an off-the-shelf module.

Taking noise considerations into account (as from the literature study), a fast response, low noise, dual-gate MOSFET was selected as the transistor to be used in the integration stage. The dual gate simplifies biasing and does not introduce additional bias circuit loading on the amplifier circuit. The specific device, a BF998 dual-gate MOSFET, is readily available and operates within the specifications on this design.

Throughout, OrCad V16.0, along with PSpice, was used for simulations. PSpice is well-known for its modeling accuracy and versatility.

Since a model of the proportional counter tube is not available in circuit simulation programs, tests and measurements as well as the counter tube's data sheet were consulted to construct a circuit that would give the same output pulse and output impedance as the counter tube. This circuit can be seen in Figure 17.

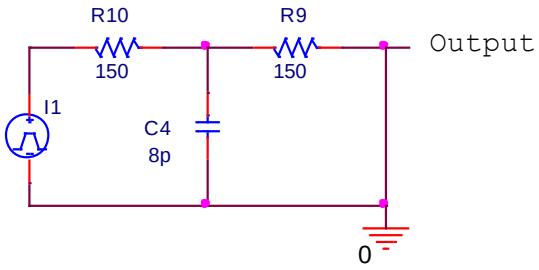

Figure 17: Circuit for counter tube simulation replacement

This simulation circuit does not significantly alter the input current pulse shape provided by the current source I_1 but when the source is loaded by the amplifier stge, it shows the same behaviour as the counter tube would.

Since the counter tube operates at high voltage, usually 1-3 kV, a high voltage filter is used between the counter tube and the preamplifier. This filter is part of the high voltage subsystem and was designed as part of the original neutron monitor. A circuit diagram for the high voltage direct current block can be seen in Figure 18.

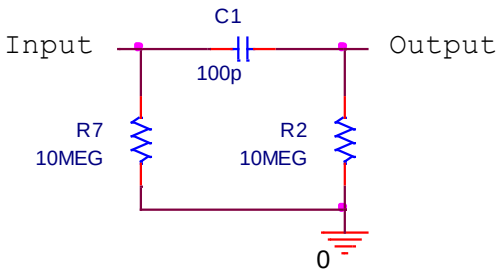

Figure 18: High-voltage DC blocking

4.3.1 Amplifier design

The charge-sensitive amplifier circuit, divided into functional blocks for the sake of analysis can be seen in Figure 19.

Functional description:

1. Block 1: Proportional counter tube equivalent circuit;
2. Block 2: High-voltage DC block;
3. Block 3: Input protection;
4. Block 4: Input resistance and dominant capacitance;
5. Block 5: Integrating gain stage with capacitive feedback and MOSFET;
6. Block 6: Final gain stage with BJT common emitter amplifiers.

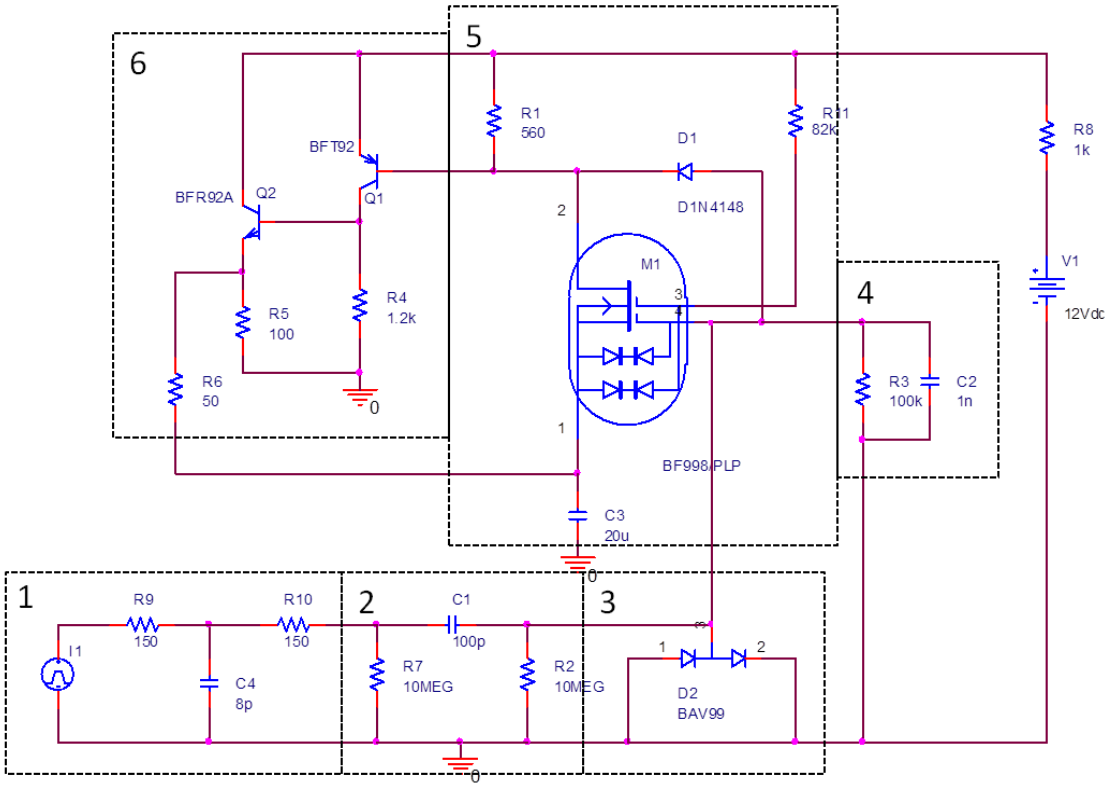

Figure 19: Amplifier circuit divided into functional blocks

Block 1 simulates the input pulse that is provided by the proportional counter tube as shown in Figure 15. A simple current pulse source is used along with the equivalent capacitance and resistance of the counter tube.

Block 2 is the high voltage blocking circuit as shown in Figure 16, thus acting as AC coupling between the high voltage tube and the preamplifier circuit. This design was inherited from the previous amplifier design.

Block 3 consists of a diode D_2 that acts as a clamping diode to protect the input against high voltage inputs. The effect of capacitance was found to be negligible and can be ignored for all practical purposes.

Block 4 consists of components R_3 and C_2 that provide a DC reference and define a dominant input capacitance. R_3 provides DC reference for the MOSFET gate, and C_2 is set as the dominant input capacitor, reducing minor effects that small external (stray) capacitors might have on the circuit.

Block 5 shows the integration stage of the amplifier. The BF998 dual-gate MOSFET is used in a common source configuration. The resistor values were selected such that $V_{G2\text{-}S} \approx 1/2V_{dc}$.

The basic design equations are obtained from first principles. For the integrating amplifier stage, a charge of 3.3 pC must be amplified to provide an output voltage proportional to this charge.

Diode D_1 is thus used as the feedback capacitor instead of using a conventional parallel combination of capacitor and resistor. This gives a feedback capacitance in the range of 0.82 – 0.85 pF. For the 1N4148 diode, with a reverse potential of around 5 V, a capacitance value of 0.85 pF was obtained.

The gain of this stage was determined by means of simulations to be ≈ 4.5 mV/pC. The final BJT stage will amplify and buffer this signal.

From a practical point of view, pre-selection of a suitable diode can be done to improve preamplifier quality during manufacturing, and a 2% tolerance can be achieved in this cost-effective way. Only a small number of amplifiers will be manufactured. Experience shows that diodes from the same manufacturing batch should exhibit similar characteristics – this will simplify the selection process.

Resistor R_{11} serves as a biasing resistor for M_1. All bias resistor values were chosen by using simulations.

Resistor R_1 serves as a biasing resistor for both M_1 and Q_1, and it has a significant effect on the feedback capacitance of diode D_1. Since negative feedback biasing was used for all three transistors, the value of R_1 could be adjusted without significantly affecting the bias point of the transistors. As a result, fine tuning of the feedback capacitance is possible without affecting the circuit bias significantly.

Capacitor C_3 serves as a bypass capacitor to provide a low impedance path to ground for AC signals. The capacitor also shunts R_6 to signal ground, thus increasing bandwidth due to the common resistance (50 Ω) at the emitter of Q_2.

Block 6 is the final gain stage of the amplifier. Two common emitter bipolar transistor configurations are used to amplify the voltage received from the integration stage. Q_1 is essentially a current buffer (used in a common emitter PNP amplifier circuit), and Q_2 is the main amplification stage (used in a common emitter NPN amplifier circuit configuration). Both stages provide voltage and current gain.

The value for R_4 was chosen to set the bias points of transistors Q_1 and Q_2.

Resistor R_5 is used for temperature compensation for DC biasing. The effective resistance seen by the emitter of Q2 is lowered from the 100 Ω of R_5 to R_5 in parallel with R_6 for AC signals. The lower resistance for AC signals provides an increase in bandwidth at the cost of a slight reduction in AC gain. R6 also provides a DC bias reference for the source of M_1.

The output for the simulations is measured at the node between R_{11} and R_8. R_8 also acts as the feedback bias resistor [49] to provide a stable bias point with respect to supply variation and temperature. The feedback bias configuration used in the transistor design ensures that the BJT transistors are always biased in the active region regardless of the value of Beta (β). The transistor stability using this type of bias network is generally good for most small-signal amplifier designs.

The variation on the output between R_8 and R_{11} will typically not influence the bias point since the voltage variation is very small (a 35 mV AC signal on 5 V DC).

Voltage V_1 is the DC power supply for all the transistors.

The amplifier and tube circuit schematic (with high voltage filter) is shown in Figure 20.

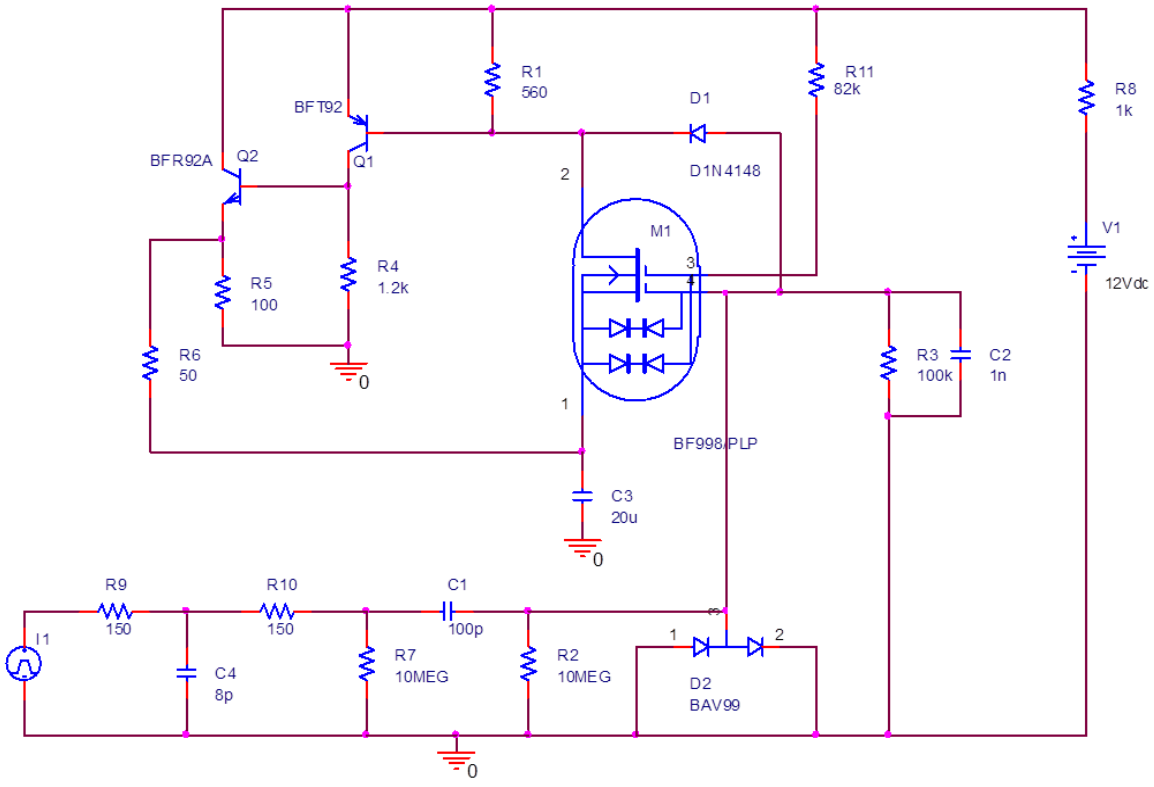

Figure 20: Circuit diagram of preamplifier with preceding filter and tube simulation

Circuit gain:

The circuit gain was determined as follows [30]:

$$Gain = \frac{V_{out\ pk-pk}}{Q},$$

with Q the amount of charge associated with the input current pulse. From the simulations, it was determined that the gain is constant for all input pulses of 3.3 pC, and was calculated to be 10,6 mV/pC.

Frequency response:

The frequency response of the circuit was simulated. The results obtained are shown in Figure 21. The -3 dB cut-off frequencies are measured as 1.5 kHz lower and around 6 MHz upper frequencies. All expected pulses fall within this frequency range as the shortest pulses have a time period of approximately 1 µs up to 7 µs. High-frequency components up to 17 x f_0 will be passed, which means the amplified triangular pulse will not be distorted.

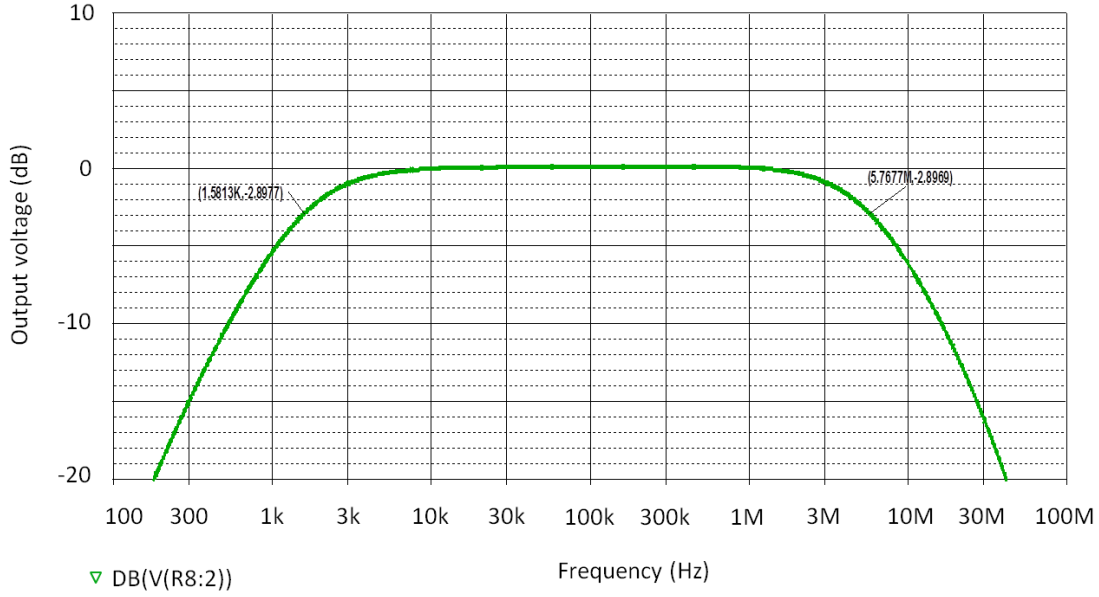

Figure 21: Simulated frequency response

Amplifier transfer:

In order to determine the amplifier transfer function, three pulses were generated. All three pulses have the same area under the curve, but with different rise and fall times to simulate fast and slow neutron occurrences. A neutron tube will generate differently shaped pulses although the detected charge is the same. The charge in each pulse is expected to be approximately 3.3 pC, as from measurements in the laboratory at the Centre for Space Research. An example of a pulse shape that is received from a $^{10}BF_3$ tube is shown in Figure 22 [47]. This pulse has been amplified (and is thus slightly rounded and elongated), but retains the general shape of the counter tube pulses.

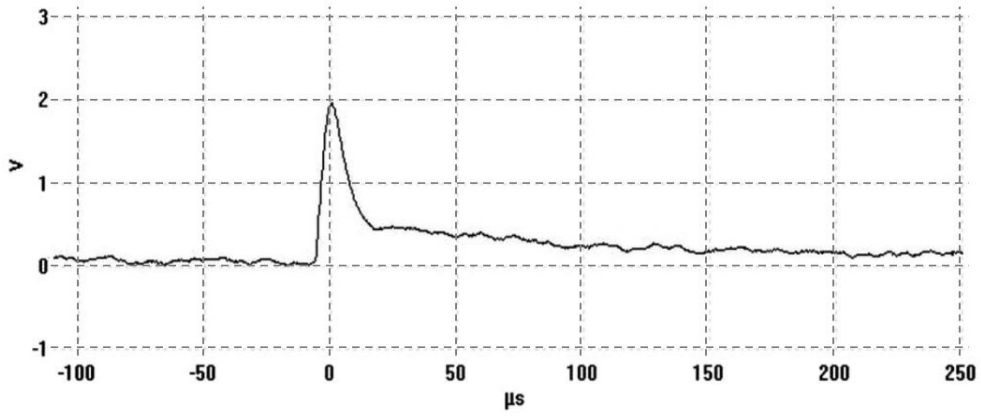

Figure 22: Single neutron pulse shape [47]

The pulse used as input to the first simulation has a peak input current of 2.2 µA, and rise and fall times of 1 µs and 2 µs respectively, as can be expected from the counter tube. This pulse was fed into the amplifier to resemble the output of the neutron tube and represents a total charge of 3.3 pC. The input current (green) and output voltage (blue) are shown in Figure 23.

From the figure it is evident that the amplifier integrates the charge (as indicated by the delayed output), after which the output decays exponentially. Note that the peak output value is proportional to the total charge of the input pulse.

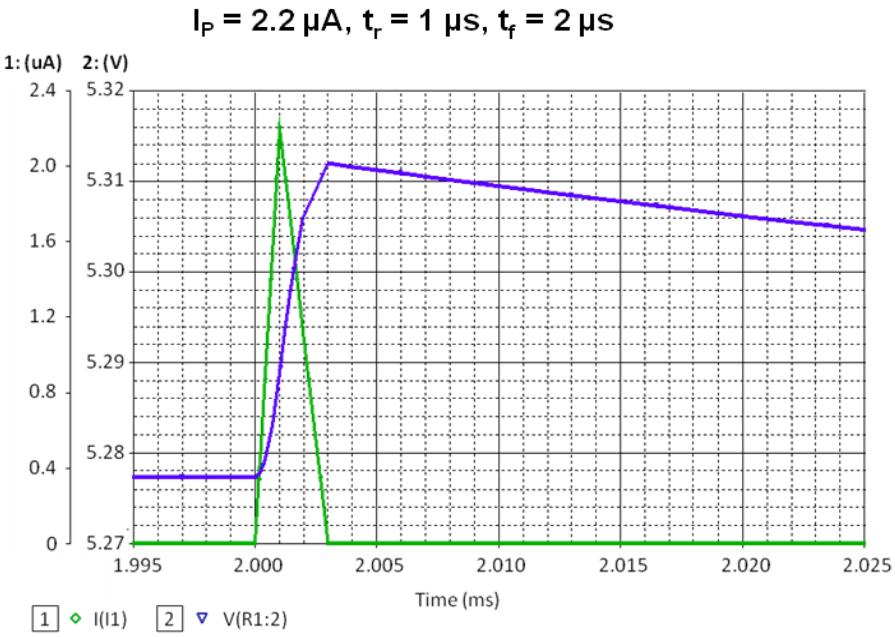

Figure 23: Graph of input current and output voltage for first simulation

The second simulation has a peak input current of 1.32 µA, and rise and fall times of 2 µs and 3 µs respectively. The pulse was fed into the amplifier circuit the same way as before. The input current (green) and output voltage (blue) are shown in Figure 24.

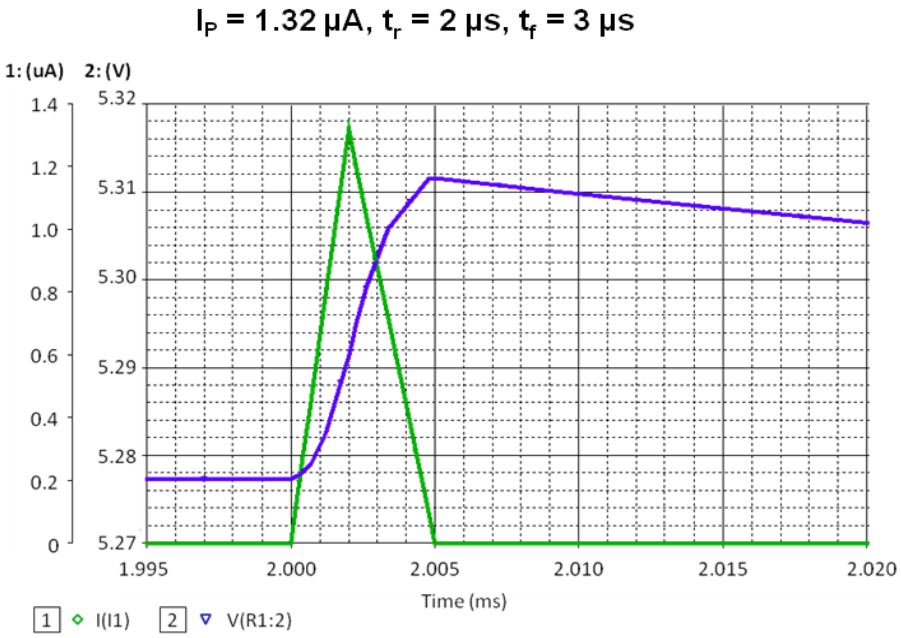

Figure 24: Graph of input current and output voltage for second simulation

The third simulation has a peak input current of 0.943 µA, and rise and fall times of 3 µs and 4 µs respectively. The input current (green) and output voltage (blue) are displayed in Figure 25.

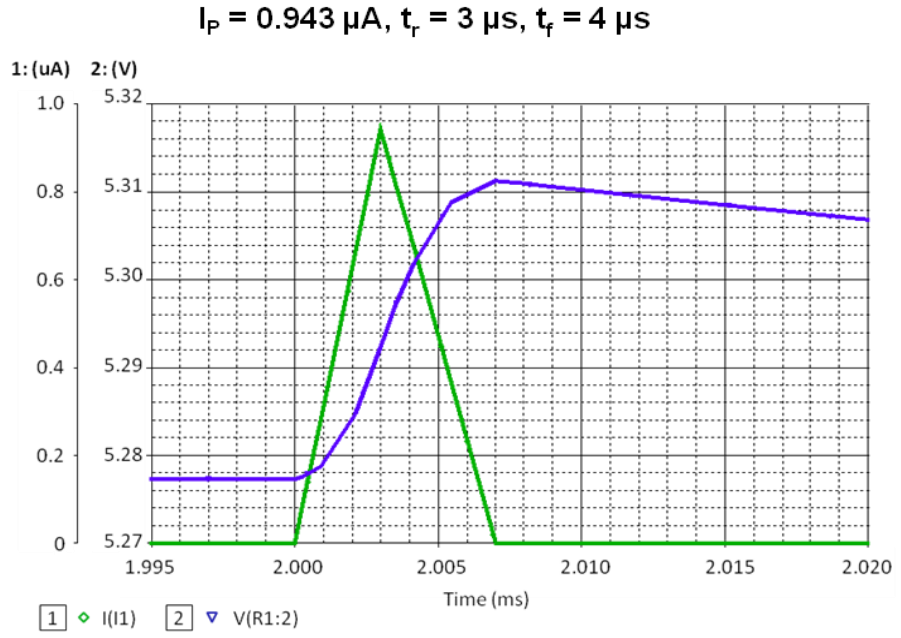

Figure 25: Graph of input current and output voltage for third simulation

The peak to peak height of the output signal is approximately 34 mV in each case with a 0.6 mV height variation between the longest and shortest pulse. The results are summarised in Table 1.

Table 1: Summary of results from Figure 23-25

Input			Output	
I_P (µA)	t_r (µs)	t_f (µs)	V_{p-p} (mV)	t_r (µs)
2.2	1	2	34.6	3
1.32	2	3	34.3	4.8
0.943	3	4	34	7

Figure 26 shows the same output as shown in Figure 23, but the time scale is longer so the characteristics (decay time and period) of the output can be observed.

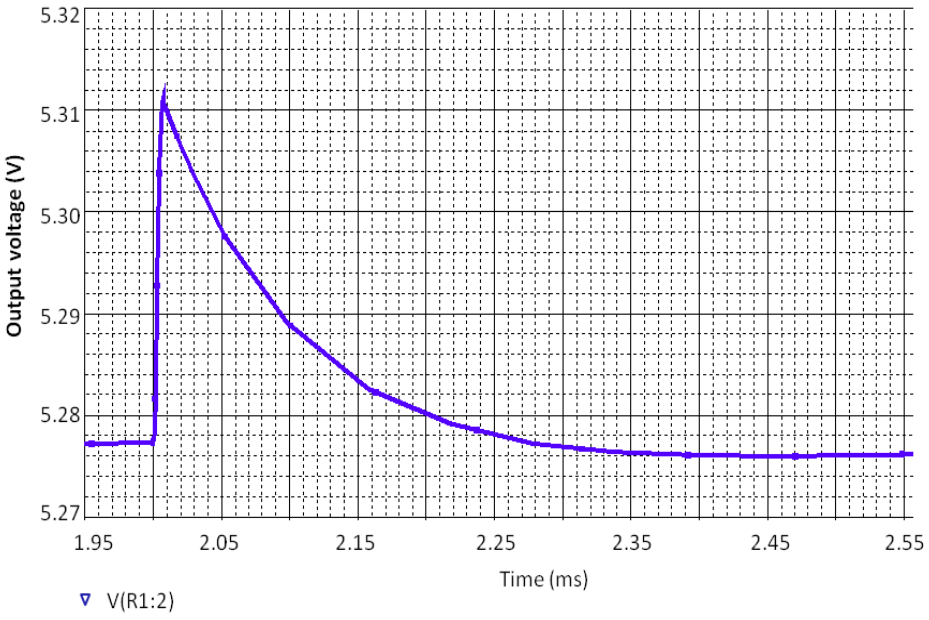

Figure 26: Amplifier output pulse shape

A simulation was run to observe the effect of two pulses occurring very close together. The result is shown in Figure 27.

The decay time from 90 % to 10 % of the peak value is measured to be approximately 200 µs. Since the mini neutron monitor generally counts 160 pulses per minute, with pulse duration around 7 µs long, it means that only 2 to 3 events occur per second, leaving an average of 300 ms between events. The second pulse can be neglected by the microprocessor that registers and counts the pulses.

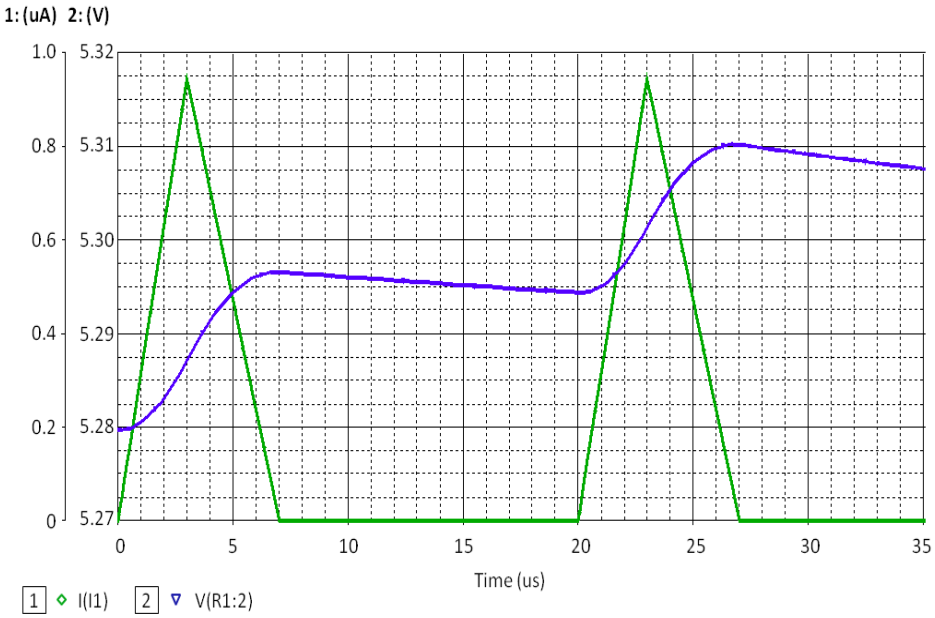

Figure 27: Graph of input current and output voltage for pulses occurring close together

Noise:

A simulation was done to measure the amount of noise on the output of the amplifier. The results are given in Figure 28.

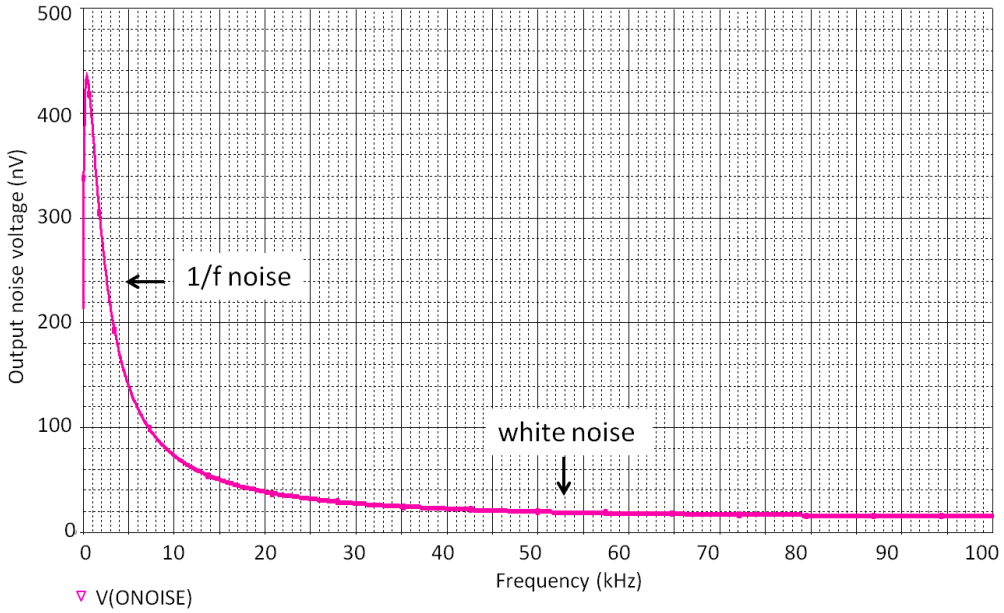

Figure 28: Output noise simulation results

The effect of 1/f noise is evident in the graph. The noise is measured to have a peak value of approximately 400 nV at about 450 Hz, that decreases exponentially up to 40 kHz. Beyond 40 kHz white noise (thermal and shot noise) is dominant and their combined effect is measured to be less than 20 nV.

When considering the SNR in the frequency range of the pulses we are expecting to receive from the counter tube, the expected pulse durations of 1 µs to 7 µs translate to 140 kHz to 1 MHz. A guard band can be included to ensure no pulses are distorted, giving a range of 100 kHz to 2 MHz. In this frequency range only thermal and shot noise are present with a combined amplitude of 20 nV RMS. The SNR can then be calculated using the following expression:

$$SNR = 20 \log \frac{V_{out}}{V_{noise}}. \quad (5)$$

This gives a SNR of 127 dB. This value is sufficiently high, therefore noise in this frequency range can be ignored. To eliminate the effect of 1/f noise, a band-pass filter can be used to filter the unwanted frequency bands.

OrCad PSpice V16.0 has very accurate noise models. Therefore, this simulation is considered to be sufficient to show the acceptably low noise that resulted from the design choice – that is, the selection of a MOSFET as the active component of the integrating amplifier.

Linearity:

A simulation was run where the linearity of the preamplifier was tested. Since small current pulses cannot be generated easily, an equivalent voltage source was applied to the input of the high voltage blocking circuit (Block 2). From these simulations, it was found that voltage pulses below 60 mV provide equivalence with respect to total charge up to 6 pC (a 10 µs input pulse with a 1.2 µA peak current gives a 60 mV output pulse with a 10 µs pulse duration – this is a worst-case condition).

A pulse duration range of 1 µs to 10 µs was used for this simulation. The input pulse amplitude and width was thus varied from 0 to 60 mV and 1 µs to 10 µs respectively. The results are given in Figure 29.

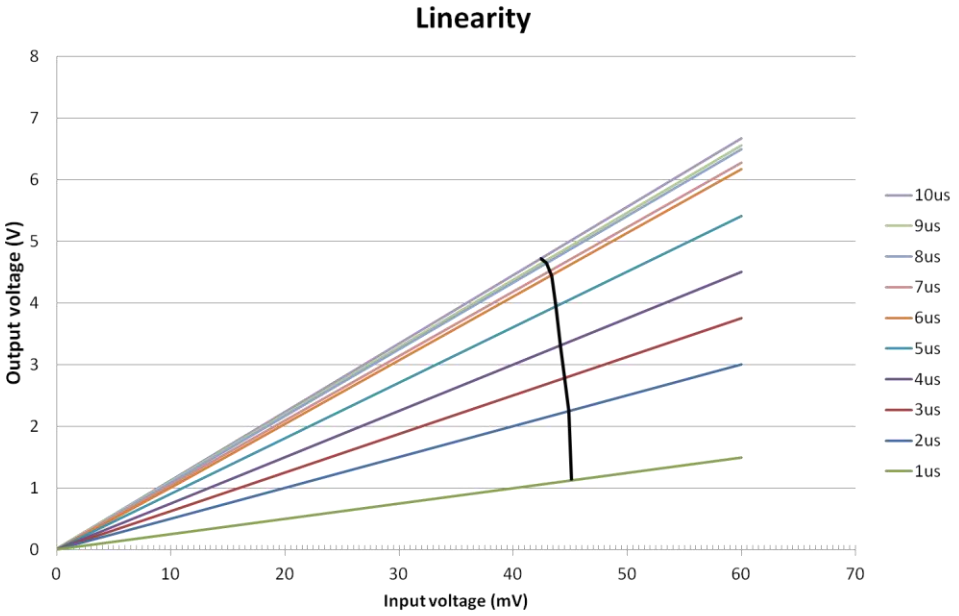

Figure 29: Linearity simulation results

It can be seen from the graph that the amplifier shows a linear response for the entire range of simulated input pulses. The black line indicates the 4.5 pC point for each pulse duration. To ensure the expected 3.3 pC is included in the linear range, this is the minimum range for which the amplifier has to respond linearly.

Please take note that the output was amplified as was also done in practical measurements later on – this is to improve the accuracy of measurement. Linearity is observed from the graph, so no scientific integrity was lost in amplifying the output.

Temperature effects:

Since the neutron monitor may be exposed to slight temperature changes during operation, a simulation was run to observe the effect of temperature on the amplifier. It is important to note that the counter will operate at room temperature (25 °C), and variations of up to 10 °C above and below this nominal value can be expected.

In order to ensure the effects of temperature are made visible, a simulation was run for temperatures of -10 °C to 50 °C at 10 °C intervals. The result is shown in Figure 30.

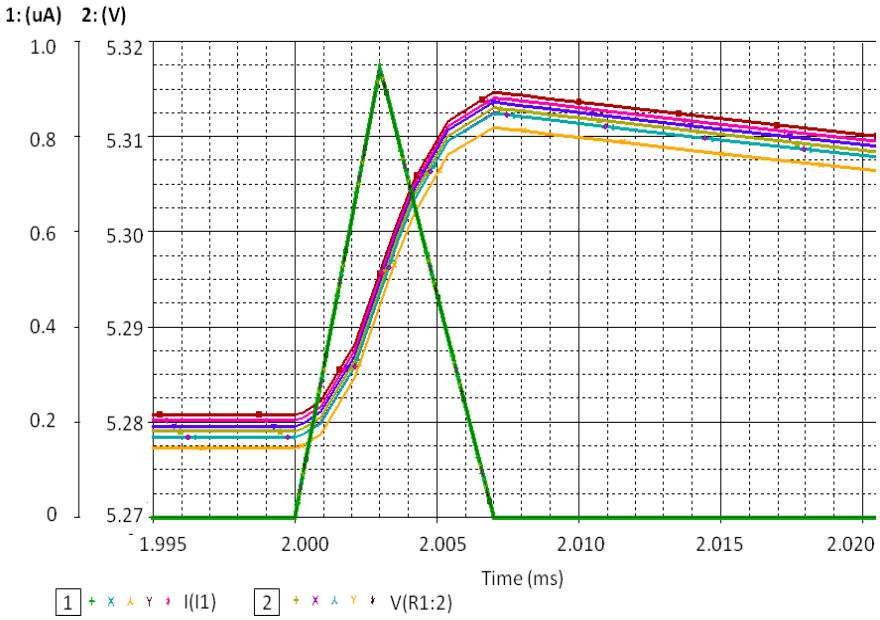

Figure 30: Simulation of temperature effects

As can be seen from the graph, the output voltage offset varies with temperature change. At the peak voltage point, the offset is measured as 2.9 mV between the highest and lowest output graphs. The results are summarised in Table 2.

Table 2: Summary of temperature simulation results

Temperature (°C)	V_{P+} (V)	V_{P-} (V)	% offset
-10	5.3144	5.2804	8.43
0	5.3138	5.2798	6.7
10	5.3126	5.2786	3.33
20	5.3115	5.2775	0.05
30	5.3115	5.2775	0
40	5.3116	5.2776	0.1
50	5.3127	5.2787	3.6

The variation in output voltage with temperature change is plotted in Figure 31.

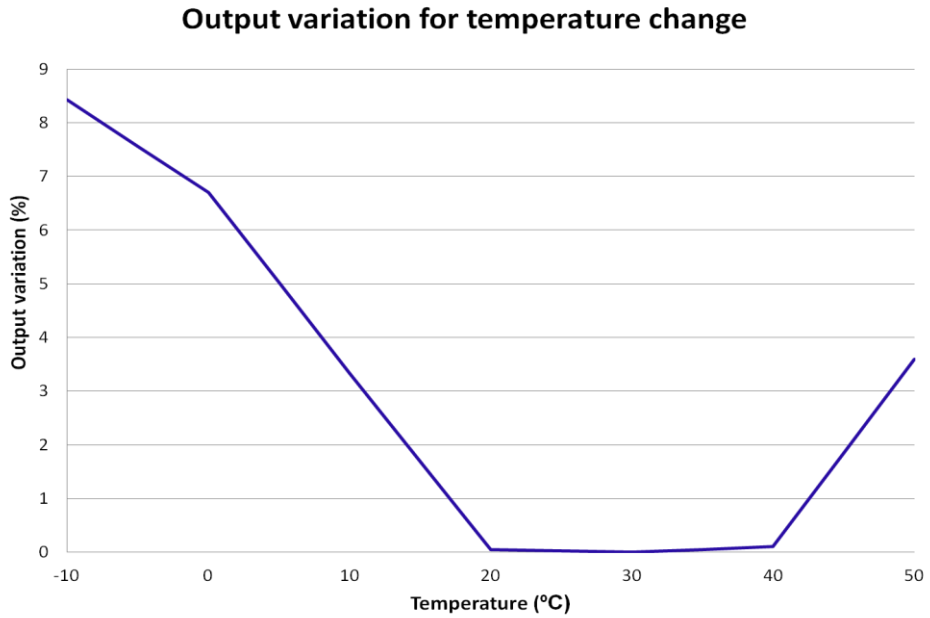

Figure 31: Graph of output variation with temperature change

Since the neutron monitor also measures and registers the temperature, the variation shall be compensated for in the microprocessor program code. It is, however, a more optimal solution to keep the ambient temperature of the environment, in which the neutron monitor is, at a constant value. Nonetheless, temperature correction will definitely be possible with the characterisation as shown above.

It is accepted that the PSpice modelling of temperature for low-level physical electronic devices is accurate due to the fact that PSpice uses detailed device physics - the above simulation results are thus considered sufficient and accurate for this research.

Sensitivity:

A sensitivity analysis was performed to identify the components that have parameters critical to the technical performance measures of the circuit design. This simulation examines how much each component affects circuit behaviour by itself, and how much variation each component causes relative to the other components. Such an analysis varies all tolerances to create worst-case (minimum and maximum) output values. The sensitivity analysis results can be used to identify which components affect yield the most, then the tolerances on those components can be lowered while the tolerance specifications of non-sensitive components can be relaxed. This information can be used to evaluate yield versus cost trade-offs.

A sensitivity analysis displays the absolute sensitivity or the relative sensitivity of a component. Absolute sensitivity is the ratio of change in a measurement value per one unit positive change in the component parameter value. Relative sensitivity is the percentage of change in a measurement based on a one percent positive change of a component parameter value.

Since capacitor and conductor values are much smaller than one unit of measurement (Farads or Henries), relative sensitivity is the more useful calculation. Relative sensitivity calculations determine the measurement change between simulations with the component parameter first set at its original value and then changed by S_v percent of its positive tolerance. This approach reduces numerical calculation errors related to small differences.

The formula used to calculate the relative sensitivity is:

$$\frac{M_s - M_n}{S_v T} \quad , \tag{6}$$

and the formula used to calculate the absolute sensitivity is:

$$\frac{M_s - M_n}{P_n S_v T} \quad , \tag{7}$$

where:

- M_s = the measurement from the sensitivity run for that parameter;
- M_n = the measurement from the nominal run;
- T = relative tolerance of the parameter;
- P_n = nominal parameter value;
- S_v =sensitivity variation.

Positive sensitivity implies that for a unit increase in the component value, there is an increase in the measurement value. If the absolute or the relative sensitivity is negative it implies that for one unit positive increase in the parameter value, the measurement value increases in the negative direction. It can also be that for a unit decrease in the parameter value, there is an increase in the measurement value.

Each component is given a tolerance of 10% and the sensitivity variation is set to 40% for the purpose of this test. The results can be seen in the table below.

Table 3: Relative sensitivity

Component	Original	Min	Max	Relative Sensitivity (%)
C_1	100 pF	90 pF	110 pF	17×10^{-6}
C_2	1 nF	1.10 nF	900 pF	-138×10^{-6}
C_3	20 uF	18 uF	22 uF	119×10^{-9}
R_1	560 Ω	504 Ω	616 Ω	-8×10^{-3}
R_2	10 MΩ	9 MΩ	11 MΩ	119×10^{-9}
R_3	100 kΩ	90 kΩ	110 kΩ	35×10^{-6}
R_4	1.20 kΩ	1.08 kΩ	1.32 kΩ	5×10^{-3}
R_5	100 Ω	90 Ω	110 Ω	25×10^{-3}
R_6	50 Ω	45 Ω	55 Ω	3×10^{-3}
R_7	10 MΩ	9 MΩ	11 MΩ	3×10^{-6}
R_{11}	82 kΩ	73.8 kΩ	90.2 kΩ	-119×10^{-9}

Since the circuit uses capacitors in the pico-Farad range, the absolute sensitivity values are not considered.

As can be seen from the relative sensitivity values in the table, the output is most dependent on the variance in value of R_5, followed by R_1, R_4, and R_6 respectively. The highest sensitivity dependence of 25 $\times 10^{-3}$ % translates to an output voltage variance of less than 0.01 mV. This indicates that the output does not have a strong sensitivity to any of the component tolerances.

The most critical capacitor in the circuit is the feedback capacitor, and care shall be taken in the selection of diodes to ensure that the 1 % tolerance level is met. That is,

the quality of the circuit will be controlled by means of manufacturing controls rather than through design controls alone.

Monte Carlo analysis:

A Monte Carlo analysis predicts the behaviour of a circuit statistically when part values are varied within their tolerance ranges. A nominal value for each measurement is calculated using the original parameter values. After the nominal runs, the value of each variable parameter is randomly calculated based on its tolerance and a flat (uniform) distribution function.

For each profile, the simulation uses the calculated parameter values, evaluates the measurements, and saves the measurement values. The calculations are repeated for the specified number of runs, after which the statistical data for each measurement is calculated. The probability density graph of the Monte Carlo simulation results is shown in Figure 32.

The average measurement value based on all run values, also known as the mean, is measured as 5.3 V, and the standard deviation is given as 4.0 mV.

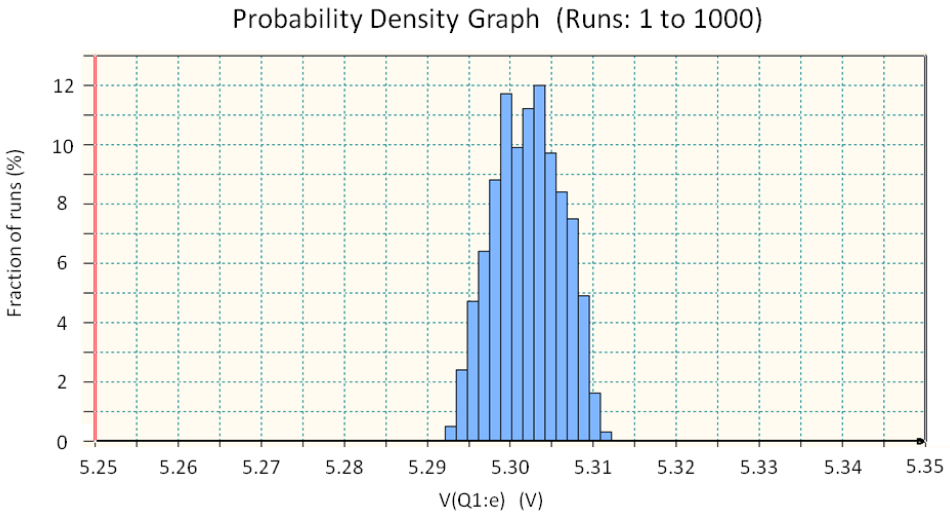

Figure 32: Monte Carlo simulation results

The 3-σ and 6-σ values can be obtained from the mean and standard deviation values, giving a 3-σ value of 12 mV, and 6-σ of 24 mV. All measurements fall within the range of both ± 3-σ and ± 6-σ from the mean.

4.4 Amplifier physical construction

From the simulation schematic, a printed circuit board (PCB) layout was designed and manufactured. The printed circuit board layout and component placement diagram can be seen in Figure 33 and Figure 34 respectively.

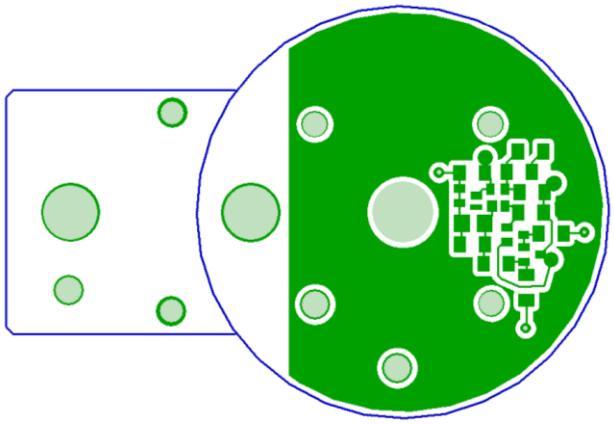

Figure 33: PCB layout for charge amplifier

The shape and size of the PCB design, one of the real-world requirements, was inherited from the previous preamplifier design.

Surface-mount devices (SMD) with the lowest possible tolerances were used to construct the circuit. Using SMD components causes very little extra space to be taken up between the tube and the amplifier, minimising incoming environmental noise. It also ensures that the amplifier will fit in the specified space within the new neutron monitor system.

The high-voltage filter consists of the high-voltage capacitor (C_1) and a 1 % tolerance through-hole resistor (R_7). Since high voltage has a tendency to arc, components C_1 and R_7 were placed away from the conductive areas on the circuit board. The required separation distance, as specified, provides for an isolation of 4 kV.

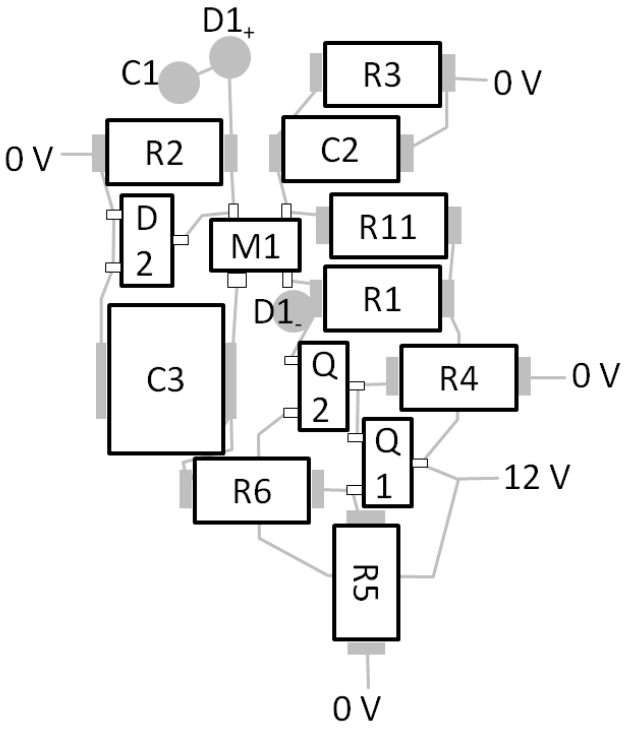

Figure 34: Component placement diagram

To reduce electro-magnetic susceptibility, the entire amplifier circuit, including the high voltage filter, will be shielded with a metal cover.

4.5 Summary

This chapter showed the details of the synthesis and design process of the charge-sensitive amplifier. Since the amplifier will be used in a real-world application, it was required to show that the design addresses requirements as obtained from an analysis of the real-world problem.

A list of requirements as set by the neutron monitor system was formulated and included the following:

- *Pulse shape requirements;*
- *Electrical interface requirements;*
- *Power consumption and power supply requirements;*
- *Noise characteristics (sources, spectrum, measurements);*
- *Linearity;*
- *Rise-time and decay-time constants;*
- *Temperature stability and other environmental robustness figures;*
- *Physical form factor and interface requirements.*

By addressing the real-world requirements, the *charge-sensitive amplifier artefact was validated*. Simulations formed part of the design process and were used to select an amplifier topology that was used to physically construct a charge-sensitive amplifier. The simulation experiments conducted were also used to characterise and evaluate the charge-sensitive amplifier. The simulations included the following:

- *Transfer function;*
- *Noise;*
- *Linearity;*
- *Temperature sweep;*
- *Sensitivity;*
- *Monte Carlo tolerance analysis.*

After the simulations provided satisfactory results, the circuit schematic was used as input for the design and construction of a printed circuit board layout. Using surface-mount devices, except for the high-voltage filter components, the circuit was constructed and shielded by a metal shield from the existing amplifier housing.

5. Experimental measurements

In this chapter the experimental methods and results that were used to evaluate the charge-sensitive amplifier are discussed.

5.1 Introduction

Two experiments were conducted to determine the characteristics of the physical charge-sensitive amplifier. Measurements from these experimental setups were used to verify selected simulation results. As a result, it can be stated that *verification is achieved when these physical measurements* of the charge-sensitive amplifier's linearity and functional capability (the pulse-height distribution) *match simulation or theoretical (where applicable) values*.

5.2 Experiment 1: Linearity

5.2.1 Purpose

The linearity of the preamplifier was tested to show that the artefact is functional and will be able to amplify without distortion. Using a function generator to simulate different input pulses received from a counter tube, the output pulses of the amplifier were measured using a Picoscope oscilloscope. From the datasheet, the recommended operating voltage of the counter tube was obtained.

5.2.2 Experimental method

The equipment used in the experiment is as follows:

- Personal computer (PC);
- Picoscope oscilloscope;
- Preamplifier with power supply/rectifier unit;
- Function generator;
- 0-30 V power supply.

The test equipment was set up as specified in the block diagram below:

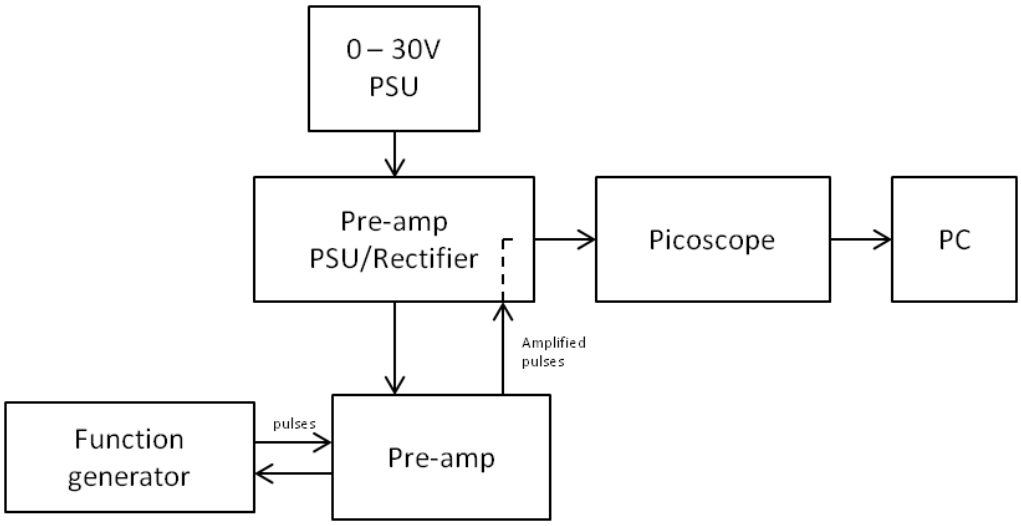

Figure 35: Block diagram of hardware setup for linearity testing procedure

The computer used needs to be running the following programs:

- Win XP / Win 7 operating system;
- PicoScope software (found on PicoScope CD or online);
- MS Excel, MATLAB, or similar.

The function generator should be set to give a triangular wave as output.

For a constant input pulse duration, the pulse height was varied and the preamplifier output pulse response was observed. This was repeated for different pulse durations.

5.2.3 Results

The results for the linearity tests can be seen in Figure 36.

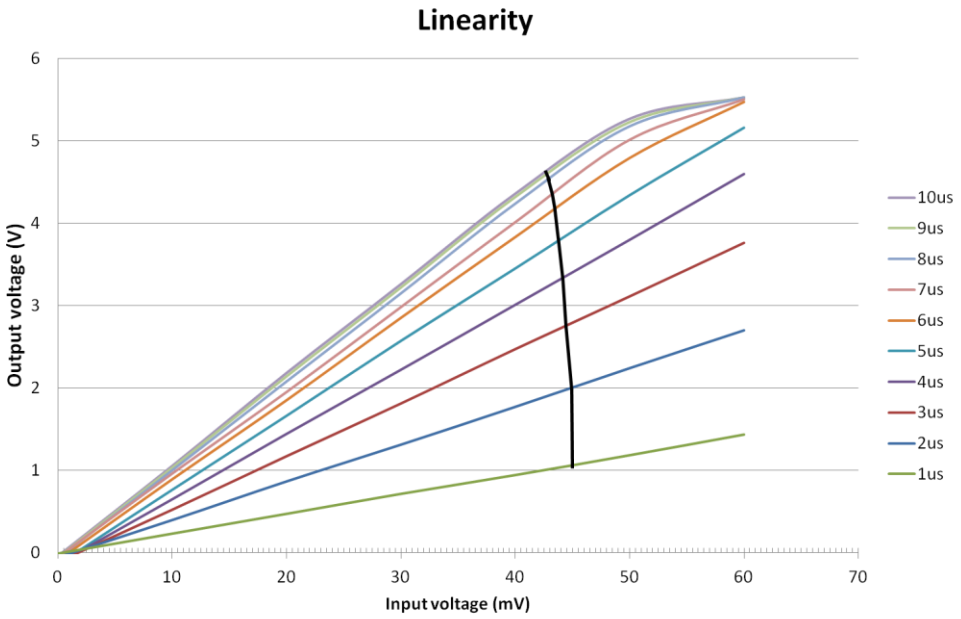

Figure 36: Linearity results of charge-sensitive amplifier

5.2.4 Analysis of results

As can be seen from the graph, the amplifier has a linear response for pulses of 1 µs to 6 µs for the entire test input voltage range, 0 to 60 mV. The output behaves nonlinearly around 50 mV test input for the 7 µs to 10 µs pulses. This corresponds to a total charge of around 4.5 pC. The 4.5 pC point for each pulse duration is indicated by the black line. It is clear that a linear response for all inputs to the left of the line is obtained. Pulses from the proportional counter tube do not exceed 7 µs in length, so the linear range of the amplifier covers the common range of pulses from the proportional counter tubes used.

When comparing this result to the results found from simulations (see Figure 29), it is seen that the simulation and experimental results differ slightly for 7 µs to 10 µs pulses above 50 mV. However, these pulses fall outside the operating range.

5.3 Experiment 2: Pulse-height distribution

5.3.1 Purpose

The charge-sensitive amplifier was connected to a neutron monitor test setup in order to measure the pulse-height distribution. The purpose of this measurement is to determine how closely the artefact represents the pulse-height distribution of the counter tube according to the tube manufacturer's datasheet. This measurement is a statistical measurement where a large number of events are generated by a neutron source, pulses are generated by a neutron tube, and are then amplified using the artefact. The resulting pulse amplitudes are measured and a pulse-height distribution is created.

To provide a large number of pulses (sample distribution) in a short sample period, a neutron source was placed close to the counter tube. The counter tube was also placed in-between two layers of wax to act as a moderator.

Two software programs were developed to analyse the sampled data and Microsoft Excel was used to graph the pulse-height distribution graph.

5.3.2 Experimental method

The following equipment was used:

- Personal computer (PC);
- Picoscope oscilloscope;
- Preamplifier with power supply/rectifier unit;
- $^{10}BF^3$ Counter tube;
- 0-30 V power supply with output cables;
- High voltage power supply with output cables.

The test equipment was configured as specified in the block diagram below.

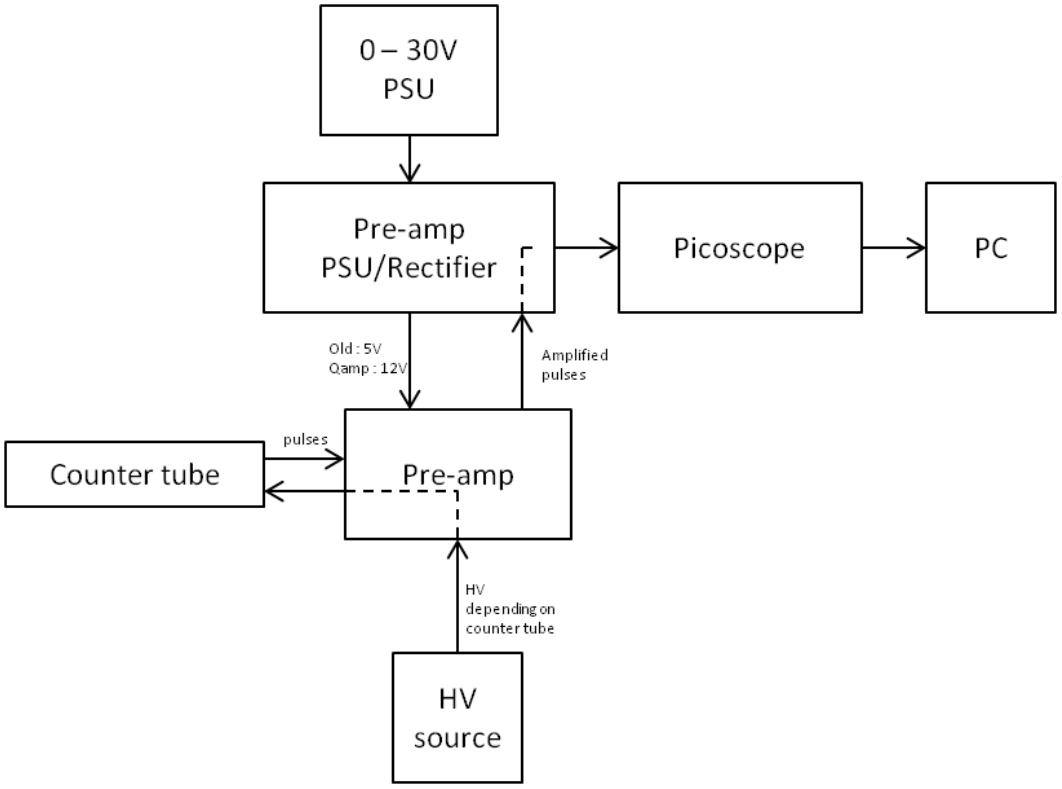

Figure 37: Block diagram of hardware setup for pulse-height experimental testing procedure

It is important to take note that, for noise reduction, the negative terminal of the 0-30 V power supply was also connected to the outside of the high-voltage source's positive or negative terminal, as well as to the negative output of the high-voltage source. This provided a common / reference ground.

The following software was used on the computer:

- Win XP / Win 7 operating system;
- PicoScope software (found on PicoScope CD or online);
- Notepad++;
- DevCpp or a similar C compiler;
- MS Excel, MATLAB, or similar.

The PicoScope software setup was defined as follows:

- Collection time: total time = 100 μs *;
- Horizontal zoom = x 1;
- Number of samples = 100 S *;
- Make buffer index very large, e.g. 1000;
- Trigger = repeat, rising edge for positive pulses , set trigger level to appropriate value e.g. 10 mV for positive pulses and noise cut out;
- Set Alarm to save current buffer as .csv (remember to tick 'enable alarm' box at bottom of menu).

* Note: 100 μs total time at 100 samples per total time provided 1 μs samples.

The DevCpp program procedure was as follows:

- Copy max_val.c, max_val.dev (or min_val if pulses are negative), pha4.c, pha4.dev to the folder where samples were saved;
- Open max_val.dev (or min_val.dev, depending on the polarity of the pulses). This program finds the maximum (or minimum for the min_val case) value of the text file created each time a pulse is registered. These maximum values are then, in turn, saved to another text file, containing then only the maximum values of the amplified pulses;
- Define the file name for max/min values to be stored in;
- Change the maximum limit for *i* values (max limit for *i* depends on no of sample screens saved by Picoscope software);
- Define the filename to open (this is obtained from the .csv files as stored by Picoscope);
- Execute, compile and run the program file (max_val.c or min_val.c);
- Open pha4.dev. This is a multichannel analysis program that will count the number of pulses in each 'channel'. In this case each channel is equivalent to

1 mV. The number of pulses counted in each channel is then saved to a separate text file;

- Set file name for values to be stored in;
- Set file name for program to open (this is the file created by max/min_val.dev);
- Set count array size and *i* value depending in highest value obtained by max_val.dev;
- Execute, compile and run pha4.dev.

In the Excel environment, the following was done:

- Open blank Excel worksheet;
- Number the first column from 0 to at least the highest value obtained from max_val.dev in increments of 0.1;
- Copy data from the text file stored by pha4.dev into excel file's to the second column;
- Graph the resulting data as a pulse-height distribution using scatter plot.

5.3.3 Results

This experiment was conducted on both the older preamplifier currently being used in the neutron monitor system as well as the new charge preamplifier. In each case more than 50 000 sample pulses, excluding noise pulses - which have slightly different cut-off values for the two different amplifiers, were accumulated and graphed. The results are shown in Figure 38.

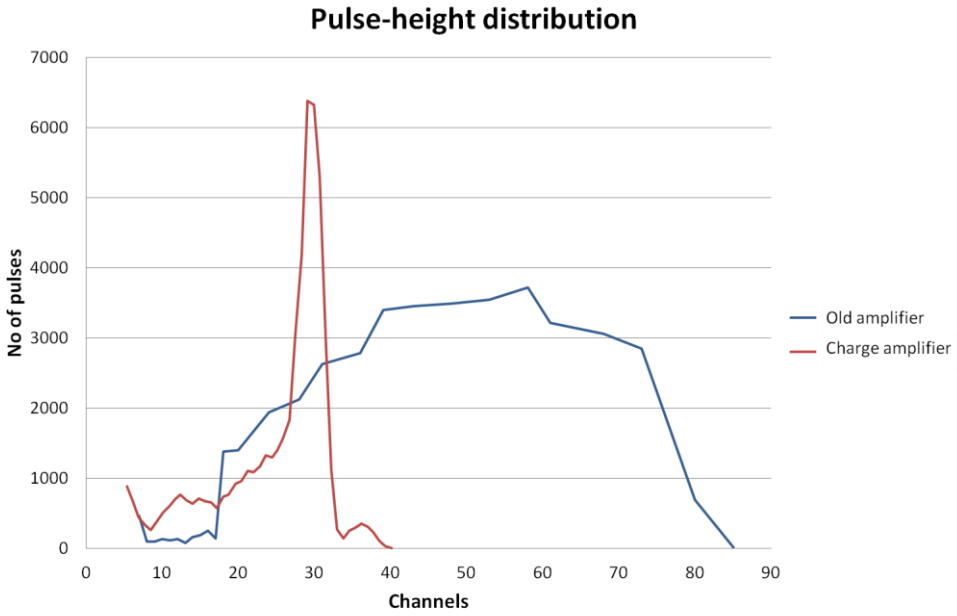

Figure 38: Pulse-height distribution of preamplifiers

5.3.4 Analysis of results

From the above figure it can be seen that the pulse-height distribution obtained by the new charge preamplifier is significantly better than the distribution obtained by the existing (outdated) preamplifier.

The full width at half the maximum height (FWHM) for the charge preamplifier graph was calculated to be 5.54 mV. The FWHM defined in the datasheet of the counter tube used is 3.67 mV (See Figure 4).

Even though there are some noise pulses present, these are distinguishable from the neutron pulses, and can be eliminated by setting a discrimination level at 5 mV.

5.4 Optimisation

For the FWHM of the experimental pulse-height distribution to match that seen in the counter tube datasheet more closely, the amplifier design was optimised by adjusting the value of the feedback capacitor (by adjusting the reverse voltage on the feedback diode through R_1). Resistor R_1 is changed in order to change the reverse voltage in order to change the junction capacitance of the diode. The changes in component values are shown below.

Component	Original value	Optimised value
R_1	560 Ω	2.2 kΩ
C_3	22 µF	1000 µF

The experiment was repeated and the results are shown in Figure 39.

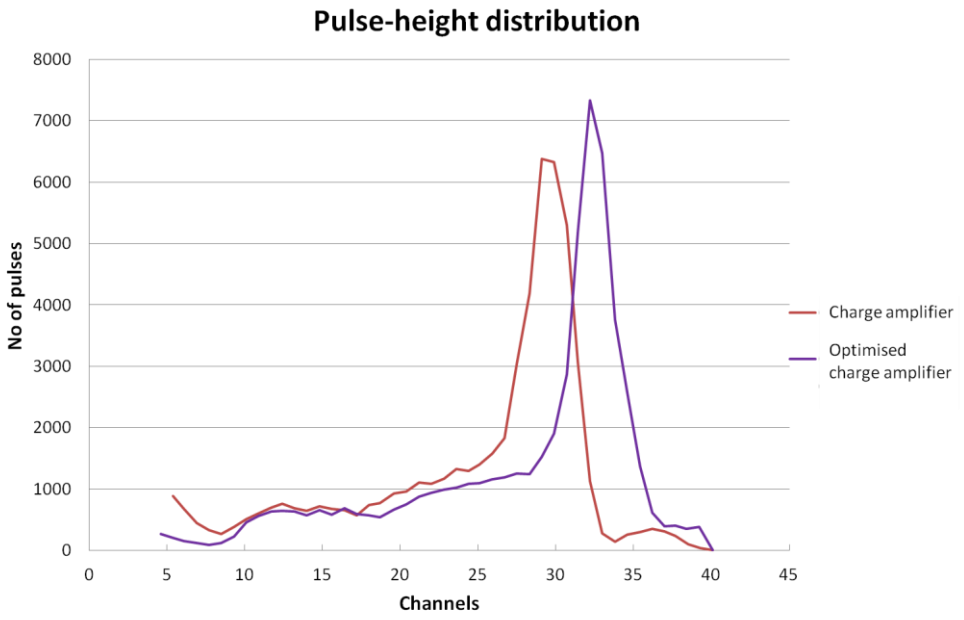

Figure 39: Pulse-height distribution of charge amplifiers

The results can be superimposed on the pulse-height distribution found in the counter tube datasheet for comparison in shape. The result is shown in Figure 40.

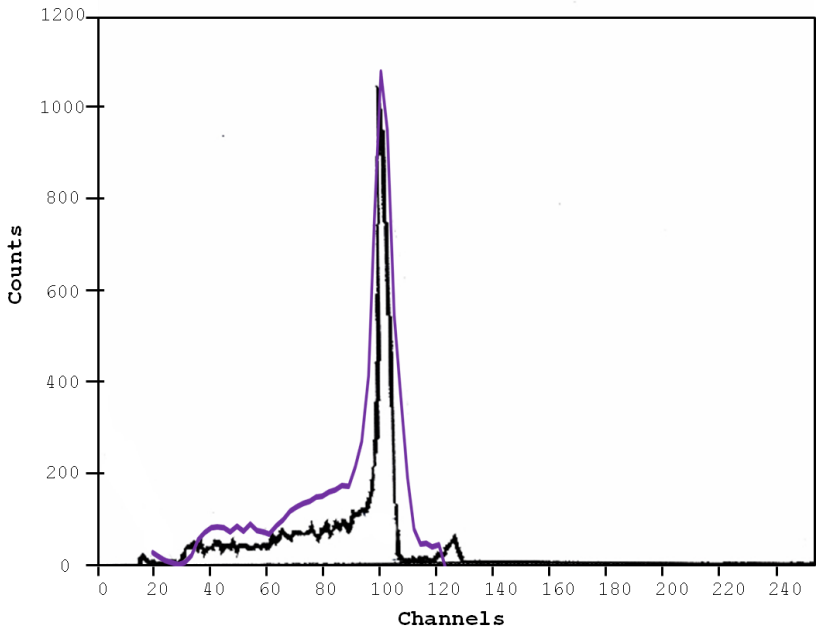

Figure 40: Optimised results superimposed on datasheet pulse-height distribution graph

The FWHM of the optimised design is calculated to be 3.74 mV, which is a 2 % difference from the 3.67 mV defined in the counter tube datasheet. This result was deemed acceptable by the Centre for Space Research.

5.5 Summary

Measurements show that the amplifier has a linear response for input pulses of length 1 µs to 6 µs for the range of up to 60 mV. For input pulses of longer duration, the amplifier reaches saturation around 50 mV.

The results also show that the pulse-height distribution obtained from the charge-sensitive amplifier has the desired shape, and the final FWHM of the pulse-height distribution graph was measured to be 3.74 mV, which is marginally

different from the 3.67 mV found in the datasheet for the ideal case. This difference is acceptable.

Through these experiments it was shown that the charge-sensitive amplifier performs as predicted by the simulations done in Chapter 4, therefore, the design of the charge-sensitive amplifier is verified by means of simulation and empirical results.

6. Summary and conclusions

This chapter shows how the research question was addressed by means of a design science research approach. A summary of the research is given, and verification and validation are discussed.

6.1 Overview

The research question:

Is it possible to synthesize an effective charge-sensitive amplifier, from first principles, that will addresses the real-world requirements of a neutron monitor system used at the Centre for Space Research of the North-West University?

was successfully addressed in this research. It was shown that the solution to this problem, namely that of synthesizing a suitable preamplifier for implementation in a neutron monitor system, was addressed.

A design science research methodology was followed to provide a framework for this research. With design science research, a real-world problem is translated into a theoretical problem, which is then solved. In parallel with the theoretical problem solution, an artefact is designed and constructed for use in the real world. Theoretical results are constantly translated into the real world to add understanding of, and value to, the real-world artefact.

For this research, a theoretical problem was thus derived from a real-world problem, and was used to formulate a research question. The theoretical problem was investigated through a literature study on neutron monitors, pulse-height

distributions of proportional counter tubes, amplifiers in general, charge-sensitive amplifiers and noise. From the literature study, the type of amplifier that would solve the pulse-height distribution problem of the neutron monitor could be selected.

Simulations aided in the design and characterisation process of the amplifier.

After satisfactory results had been obtained from the simulations, the amplifier was constructed and evaluated in a neutron monitor test setup. Experiments were conducted to answer the research question.

The initial objectives are repeated below. Each objective is discussed to show compliance.

6.2 Objective 1: Obtain different preamplifier configurations

This objective was addressed in the literature study. Different configurations of amplifiers were obtained and discussed. Operational amplifiers, transistor amplifiers (BJT and FET), and integrated circuits were identified and analysed. For a cost-effective solution, a MOSFET amplifier was selected as a low-noise first amplifier stage as it provides acceptable noise performance, design flexibility, and availability of components.

BJT amplifiers were selected as final stage amplifiers as the signal-to-noise is mostly determined by the initial amplification stage.

6.3 Objective 2: Meet requirements for the real-world artefact

The real-world requirements that were set out at the onset of this research were addressed in this research, as described in the sections that follow.

6.3.1 Pulse amplification

The preamplifier amplified pulses of 3.3 pC successfully for different pulse durations representative of an actual neutron tube. Three pulses were selected, namely:

- Pulse 1: Peak input current of 2.2 µA, and rise and fall times of 1 µs and 2 µs respectively;
- Pulse 2: Peak input current of 1.32 µA, and rise and fall times of 2 µs and 3 µs respectively;
- Pulse 3: Peak input current of 0.943 µA, and rise and fall times of 3 µs and 4 µs respectively.

The amplifier simulations showed that the pulses were amplified as per requirement. The output pulse was found to be 34 mV ± 0.6 mV for an input of 3.3 pC. The gain was found to be approximately 34 mV / 3.3 pC ≈ 10.3 mV / pC, which is sufficiently close to 10.6 mV / pC. The frequency response of the amplifier showed that all pulses in the frequency band of interest will be amplified.

6.3.2 Electrical interface

The input resistance of the amplifier was designed to be 100 kΩ, which is significantly higher than the output resistance of the counter tube, which is defined to be 300 Ω.

6.3.3 Power supply interface

The amplifier was designed to operate at 12V, with the current consumption measured as 5.7 mA. This consumption is significantly less than the 10 mA requirement.

6.3.4 Noise

A low-noise design was done, starting with a selected configuration from literature, with simulation evidence from PSpice that the selection provided sufficiently low noise of 400 nV in the region of interest. The noise is in the form of white noise, with 1/f noise playing a role at lower frequencies below the frequency band of interest.

6.3.5 Linearity

The amplifier was found to be linear for total charge of up to 4.5 pC. This is significantly higher than the specified 3.3 pC requirement. Simulations and measurements confirm this result.

6.3.6 Rise and decay time

A rise time of 1 µs was achieved, as required. The decay of the amplifier was found to be approximately 200 µs, which is significantly less than the 300 ms requirement.

6.3.7 Temperature

Simulations showed that the temperature variation is within reasonable bounds inside the operating region. A temperature simulation in PSpice was done for temperatures between -10 °C and 50 °C. A maximum deviation of around 8.5% was determined over the temperature span, but a deviation of less than 2% was measured in the region of interest. The deviation can be compensated for by means of temperature correction in the microcontroller firmware.

6.3.8 Physical form factor

The resulting artefact was designed for the existing preamplifier and thus addresses this requirement.

6.3.9 Cost and availability

The major challenge was to design this artefact for low cost. The lowest cost will be when commercial off the shelf low-noise transistors are used, which is the case in this design. A low-noise MOSFET and two low-cost BJT's were used as integrating preamplifier and output gain stages, respectively. A diode was used as feedback element to reduce cost and availability constraints associated with expensive low tolerance capacitors.

6.4 Validation and verification

Validation was achieved by addressing all functional requirements for the real-world charge-sensitive amplifier as discussed above.

Verification was achieved because the empirical results from experimentation match the results from simulations. The comparison between simulation (theoretical) and measured results for each experiment are discussed below.

Linearity: An equivalent voltage source was selected as it is exceedingly difficult to generate small current pulses in practice. Simulations were done to characterise the linearity of the circuit, and the results showed a linear output response for input pulses in the range of 1 - 10 µs, with amplitudes of up to 60 mV. Experimental results showed a linear output response for input pulses in the range 1 - 10 µs with amplitudes up to 60 mV, but with compression evident from the empirical measurements at inputs higher than 4.5 pC. However, the most important result is that a total charge of 4.5 pC still provides a linear transfer characteristic for pulses up to 7 µs, which is the worst-case condition for the neutron tube in question.

Pulse-height distribution: Using the neutron monitor test setup, an experiment was done where 50 000 output pulses were collected and graphed to construct a pulse-height distribution graph. The resulting empirical graph has a similar

distribution to that found in the counter tube datasheet. This result provides sufficient evidence that all the other results may be accepted.

Optimisation was used to adjust design parameters such that the full maximum at half minimum of the experimental pulse-height distribution matches that found in the counter tube datasheet more closely.

To conclude, the use of design science research to produce both theoretical value and real-world value has resulted in the synthesis and evaluation of a functional preamplifier. The underlying theory was thoroughly researched and mastered, and a functional artefact was created that will be employed in future generations of neutron monitors.

7. References

[1] Hevner, A., March, S. & Park, S.a.R.J., 2004. Design science in information systems research. *MIS quarterly*, 28(1), p.75–105.

[2] Iivari, J., 2007. A paradigmatic analysis of information systems as a design science. *Scandinavian Journal of Information Systems*, 19(2), pp.9 - 22.

[3] Storey, V.a.M.S., 2008. Design science in the information systems discipline: An introduction to the special issue on design science research. *MIS Quarterly*, 32(4), pp.725-30.

[4] Jordaan, P., 2013. *Synthesis and evaluation of a data management system for machine-to-machine communication*. Masters thesis. North-West University.

[5] Bahill, A.a.H.S., 2005. Requirements Development, Verification, and Validation Exhibited in Famous Failures. *Systems Engineering*, 8(1), pp.1 - 14.

[6] Clem, J., 2004. *Department of Physics*. [Online] Purdue University - Annual CRONUS collaboration meting Available at: https://www.physics.purdue.edu/cronus/files/cronus04.ppt [Accessed 14 March 2013].

[7] Bieber, J., Eroshenko, E. & Evenson, P., 2000. *Cosmic Rays and Earth*. International Space Science Institute: Springer.

[8] Fuller, N., 2009. *Neutron monitors - Neutron Monitor Database (NMDB)*. [Online] Available at: http://www.nmdb.eu/?q=node/142 [Accessed 14 October 2011].

[9] Frame, P., 2011. *Boron Trifluoride (BF3) Neutron Detectors*. [Online] Available at: http://www.orau.org/ptp/collection/proportional%20counters/bf3info.htm [Accessed 14 October 2011].

[10] Jones, G.P. & Tsorbatzoglou, K.M., 1993. Design of He-3 Neutron Detectors without the use of Polyatomic Quench Gases. In *Nuclear Science Symposium and Medical Imaging Conference, 1993., 1993 IEEE Conference Record.* Waltham MA, 1993. TGM Detectors Inc.

[11] LND Inc, n.d. *Designers and Manufacturers of Nuclear Radiation Detectors*. [Online] Available at: http://www.lndinc.com/products/category/38/ [Accessed 14 October 2011].

[12] Saint-Gobain Ceramics and Plastics Inc, 2010. *Gas filled radiation detectors: Proportionals counters*. [Online] Available at: http://www.qsl.net/k/k0ff/Proportional/Proportional/Proportional-Counters-Brochure.pdf [Accessed September 2013].

[13] Schlotz, R. & Uhlig, S., 2006. *BRUKER ADVANCED X-RAY SOLUTIONS*. [Online] Bruker axs Available at: http://www.fem.unicamp.br/~liqcqits/facilities/xrf/[Bruker_2006]%20Introduction%20to%20X-ray%20Fluorescence%20(XRF).pdf [Accessed 16 October 2011].

[14] Crane, T.W. & Baker, M.P., 1991. Neutron Detectors. *Passive Nondestructive Assay of Nuclear Materials*, pp.379 - 406.

[15] LND Incorporated, 2011. *Datasheet 402914*. Datasheet. Potchefstroon: North-West University.

[16] Jung, W., Kester, W. & Bryant, J., 2002. *Op Amp Applications*. United States of America: Analog Devices. pp.H1 - 1.128.

[17] Sze, S. & Lee, M., 2013. Bipolar transistors and related devices. In *Semiconductor devices: Physics and technology*. Asia: John Wiley & Sons. pp.123 - 229.

[18] Neamen, D., 2009. *Microelectronics: Circuit Analysis and Design*. University of New Mexico: McGraw-Hill Education.

[19] Electronics Lab, n.d. *Experimentalists anonymous*. [Online] Available at: experimentalistsanonymous.com/diy/Schematics/Miscellaneous/Op%20amps%20explained.pdf [Accessed 16 October 2011].

[20] Philips, 1988. *AN165 - Integrated operational amplifier theory (Application note)*. [Online] Cirrus Logic Available at: http://www.digchip.com/datasheets/parts/datasheet/000/AN165-pdf.php [Accessed 12 September 2011].

[21] Albaugh, N., 2000. *The Instrumentation Amplifier Handbook: Including Applications*. Tucson, Arizona: Burr- Brown Corporation.

[22] Texas Instruments, 2007. *Noise Analysis in Operational Amplifier Circuits*. Application report. Dallas, Texas: Texas Instruments Incorporated Digital Signal Processing Solutions.

[23] Zumbahlen, H., 2007. The Op Amp. In *Basic Linear Design*. Analog Devices, Inc. pp.1.47 - 1.55.

[24] Spieler, H., 1998. *Introduction to Radiation Detectors and Electronics - Noise in Transistors*. Lecture notes. Berkeley: University of California.

[25] Butler, L., 1985. Amplifier Noise. *Amature Radio - Wireless Institute of Australia*, (11).

[26] Knol, G., 2000. Linear and Logic Pulse Functions. In *Radiation Detectibn and Measurement*. 3rd ed. United States of America : John Wiley & Sons, Inc. pp.610 - 617.

[27] Webster, J., 2008. *Amplifiers and Signal Processing*. [Online] Available at: http://www.unc.edu/~finley/BME422/Webster/c03.pdf [Accessed August 2013].

[28] Zhang, Y. et al., 2012. Design of a monolithic CMOS sensor for high efficiency neutron counting. *Microelectronics journal*, pp.730 - 736.

[29] Buchman, S., Mester, J. & Sumner, T.J., 1999. Charge Measurement. *The Measurement, Instrumentation, and Sensors Handbook*, pp.44-1 - 44-11.

[30] Hamamatsu, 2001. *Characteristics and use of charge amplifier*. [Online] Available at: http://www.hamamatsu.com/resources/pdf/ssd/charge_amp_techinfo_e.pdf [Accessed July 2012].

[31] Bönisch, S. & Namaschk, et al., 2007. Charge equalizing and error estimation in position sensitive neutron detectors. *Nuclear Instrumentation Methods Physics Research A*, A570, p.133–139.

[32] Radeka, V., 1968. State of the art of low noise amplifiers for semiconductor radiation detectors. In *Procedings International Nuclear Electronics Conference*. Versaille, France, 1968.

[33] Radeka, V., 1988. Low-noise techniques in detectors. *Annual reviews of nuclear and particle science*, 38, p.217.

[34] Bertuccio, G.a.P.A., 1993. A method for the determination of the noise parameters in preamplifying systems for semiconductor radiation detectors. *Review of Scientific Instruments*, 64(11), pp.3294-98.

[35] van Esch, P., Gahl, T. & and Guerard, B., 2004. Design criteria for electronics for resistive charge division in thermal neutron detection. *Nuclear instruments and methods in physics research a*, A526, p.493–500.

[36] Bönisch, et al., 2008. Low-Frequency Noise of Resistively Coupled Charge Amplifiers. *IEEE TRANSACTIONS ON NUCLEAR SCIENCE*, 55(4), pp.2315-22.

[37] O'Connor, P. & De Geronimo, G., 2002. Prospects for charge sensitive amplifiers in scaled CMOS. *Nuclear instruments and methods in physics research*, pp.713 - 725.

[38] Smith, K.a.C.J., 1966. A Low-Noise Charge Sensitive Preamplifier for Semiconductor Detectors Using Paralleled Field-Effect-Transistors. IEEE Transactions on Nuclear Science, 13(3), pp.468-476.

[39] Bradley, A., 1966. Design for a Versatile Charge Sensitive Preamplifier for Nuclear Radiation Detectors. *IEEE Transactions on Nuclear Science*, 13(1), pp.611 - 622.

[40] Grainger, G. & Bedford, D.K., 1978. Low noise charge-sensitive preamplifier for fast pulse counting. *Electronics Letters* , 14(5), pp.126 - 127.

[41] Cremat Inc, 2013. *Cremat Inc*. [Online] Available at: http://www.cremat.com/ [Accessed September 2013].

[42] Amptek, 2013. *Amptek*. [Online] Available at: http://www.amptek.com/ [Accessed September 2013].

[43] Ametek, 2010. *Ortec*. [Online] Available at: http://www.ortec-online.com/ [Accessed September 2012].

[44] Visser, B., 2011. *Personal communication*. North-West University.

[45] Cremat, Inc., 2013. *CSP selection guide*. [Online] Available at: http://www.cremat.com/preamplifier_choice.htm [Accessed September 2013].

[46] Nakhostin, M. et al., 2013. Use of commercial operational amplifiers in a low cost multi-channel preamplifier system. *Radiation Physics and Chemistry*, 85, pp.18 - 22.

[47] Ferrarini, M., Varoli, V., et al., 2010. A wide dynamic range BF3 neutron monitor with front-end electronics based on a logarithmic amplifier. *Nuclear Instruments and Methods in Physics Research A.* 613, pp.272–276.

[48] Massarotto, M., Carlosena, A. & and Lopez-Martin, A., 2008. Two-Stage differential charge and transresistance amplifiers. *IEEE transactions on instrumentation and measurement*, 57(2), pp.309 - 320.

[49] V. K. Mehta, 2005 *Principles of Electronics: For Diploma, AMIE, Degree & Other Engineering Examinations*. S. Chand & Company Ltd.